iScience

CellPress
OPEN ACCESS

Article

IGFBP3 induced by the TGF-β/EGFRvIII transactivation contributes to the malignant phenotype of glioblastoma

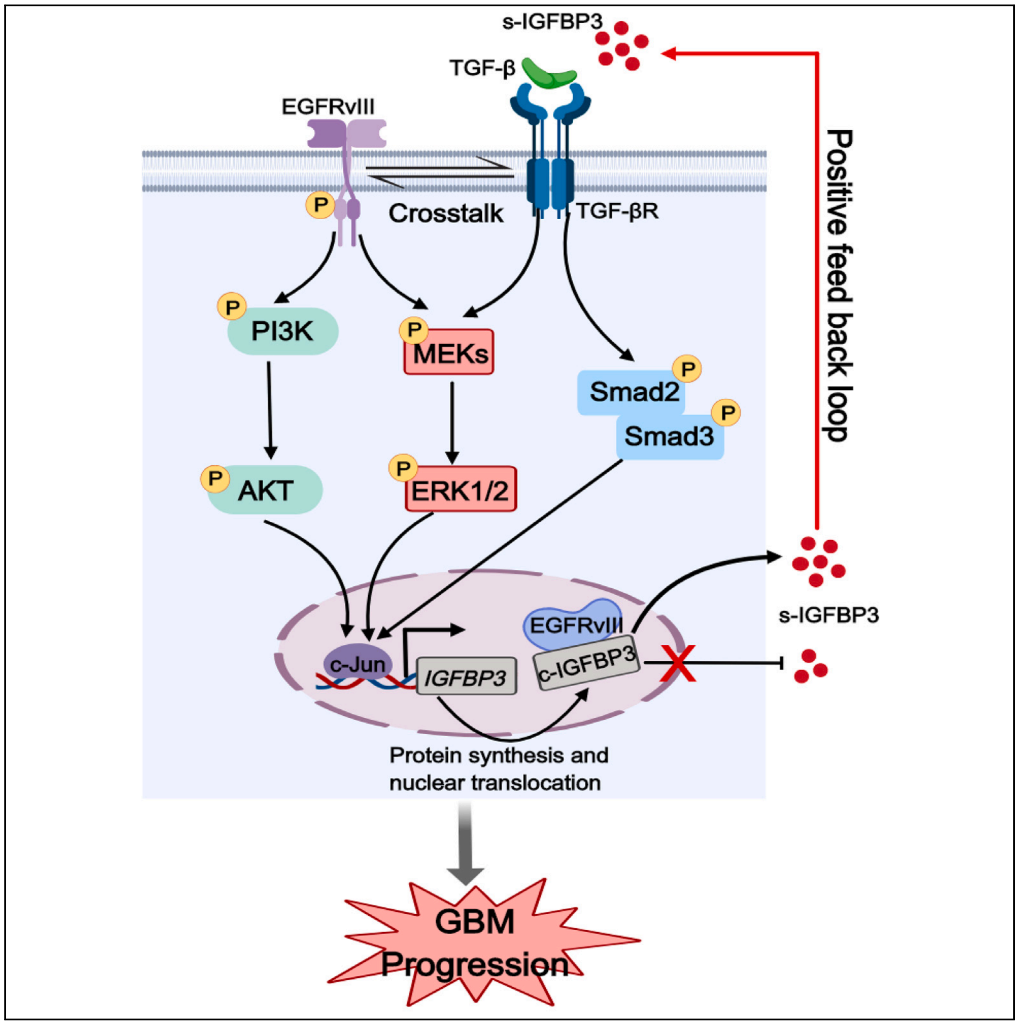

Xuehua Zhang, Guoyan Wang, Yujiao Gong, ..., Huan Ren, Xiao Zhu, Yucui Dong

renh@sustech.edu.cn (H.R.)
xzhu@ytu.edu.cn (X.Z.)
yucuidong@bzmc.edu.cn (Y.D.)

Highlights

IGFBP3 is induced by the crosstalk between TGF-β and EGFRvIII signaling in GBM cells

EGFRvIII and IGFBP3 are overexpressed and positively correlated in GBM patients

Inhibition of IGFBP3 effectively disturb the TGF-β/EGFRvIII/c-Jun/IGFBP3 axis

Targeting IGFBP3 effectively suppressed tumor growth in EGFRvIII xenografts model

Zhang et al., iScience *26*, 106639
May 19, 2023
https://doi.org/10.1016/j.isci.2023.106639

iScience

CellPress
OPEN ACCESS

Article

IGFBP3 induced by the TGF-β/EGFRvIII transactivation contributes to the malignant phenotype of glioblastoma

Xuehua Zhang,[1,10] Guoyan Wang,[2,10] Yujiao Gong,[3] Leilei Zhao,[1] Ping Song,[4] He Zhang,[5] Yurui Zhang,[1] Huanyu Ju,[6] Xiaoyu Wang,[7] Bin Wang,[1] Huan Ren,[8,*] Xiao Zhu,[9,*] and Yucui Dong[1,11,*]

SUMMARY

Dual or multi-targets therapy targeting epidermal growth factor receptor variant III (EGFRvIII) and other molecular may relax the constraint for glioblastoma (GBM), putting forward the urgent requirement of finding candidate molecules. Here, the insulin-like growth factor binding protein-3 (IGFBP3) was considered a candidate, whereas the mechanisms of IGFBP3 production remain unclear. We treated GBM cells with exogenous transforming growth factor β (TGF-β) to simulate the microenvironment. We found that TGF-β and EGFRvIII transactivation induced the activation of transcription factor c-Jun, which specifically bound to the promoter region of IGFBP3 through Smad2/3 and ERK1/2 pathways and promoted the production and secretion of IGFBP3. *IGFBP3* knockdown inhibited the activation of TGF-β and EGFRvIII signals and the malignant behaviors triggered by them *in vitro* and *in vivo*. Collectively, our results indicated a positive feedback loop of p-EGFRvIII/IGFBP3 under administration of TGF-β, blocking IGFBP3 may be an additional target in EGFRvIII-expressing GBM-selective therapeutic strategy.

INTRODUCTION

Glioblastoma (GBM) accounts for 48.3% of malignant tumors of the central nervous system (CNS). Owing to the high aggressiveness of GBM, malignant symptoms of GBM patients develop rapidly in a few days or months.[1] GBM exhibits both intra and inter-tumor heterogeneity, lending to resistance and eventual tumor recurrence.[2–4] Targeted therapy is common current therapies for GBM. High-level EGFR amplification was observed in 97% of the classical subtypes, and type vIII EGFR mutations (EGFRvIII) were found in approximately half of the typical samples analyzed.[5] Hence, EGFRvIII targeting therapy is the most common therapeutic approaches for GBM-EGFR patients.[6,7] However, therapies directed against EGFRvIII have not yet shown clear benefit clinically, possibly because of the immunosuppressive microenvironment of the GBM, and the positive feedback loop for EGFRvIII.[8] Dual or multi-targets therapy targeting EGFRvIII and other associated molecular may relax the constraint of EGFRvIII targeting therapy. Hence, further studies to identify other molecular associated with the disease progression in EGFRvIII-GBM and to clarify the underlying mechanisms are urgent.

The insulin-like growth factor binding protein family (IGFBPs) contains six different binding proteins (IGFBP1-IGFBP6), among which IGFBP3 is the main carrier of IGFs *in vivo*.[9,10] IGFBP3 belongs to a class of molecules with diverse regulatory functions[11] and plays an important role in malignancy development of cancers, including melanoma, glioma, and breast cancer.[12,13] Zhong et al. found that IGFBP3 expression accounted for 97% in GBM cell lines.[14] By exploring the level of IGFBP3 in the blood of clinical patients with GBM and its expression in GBM tissue samples, it was found that IGFBP3 could promote cell migration and invasion, cycle progression, and facilitate metastasis. IGFBP3 expression is associated with poor patient prognosis, thus IGFBP3 was identified as a novel prognostic biomarker for glioblastoma.[15–17] Moreover, EGFRvIII signaling was probably implicated in mediating IGFBP3 production. In the IGFBP3-transfected T47D cell model, the acquisition of growth stimulation associated with IGFBP3 expression was accompanied by enhanced EGFR signaling.[18] Takaoka et al.[19] demonstrated that IGFBP3 was identified as a highly upregulated gene in EGFR-overexpressing cells in patients with developing esophageal cancer. Meanwhile, it has been well recognized that transforming growth factor β (TGF-β) was closely associated with EGFRvIII signaling. TGF-β is an important component of the GBM immunosuppressive microenvironment

[1]Department of Immunology, Binzhou Medical University, Yantai, Shandong 264003, China

[2]Clinical Laboratory of Yantai Affiliated Hospital of Binzhou Medical University, Yantai, Shandong 264199, China

[3]Guangdong Provincial Key Laboratory of Biomedical Imaging, The Fifth Affiliated Hospital of Sun Yat-sen University, Zhuhai, Guangdong 519000, China

[4]Department of Ophthalmology, Jiarun Hospital of Harbin, Harbin, Heilongjiang 150000, China

[5]Department of Immunology, Qiqihar Medical University, Qiqihar, Heilongjiang 161000, China

[6]Department of Immunology, Harbin Medical University, Harbin, Heilongjiang 150081, China

[7]Department of Neurology, Hongda Hospital, Jinxiang, Shandong 272200, China

[8]School of Medicine, Southern University of Science and Technology, Shenzhen, Guangdong 518000, China

[9]School of Computer and Control Engineering, Yantai University, Yantai, Shandong 264005, China

[10]These authors contributed equally

[11]Lead contact

*Correspondence: renh@sustech.edu.cn (H.R.), xzhu@ytu.edu.cn (X.Z.), yucuidong@bzmc.edu.cn (Y.D.)

https://doi.org/10.1016/j.isci.2023.106639

that promotes invasion, angiogenesis as well as suppression of the immune system.[20] Recent studies have suggested that TGF-β can also induce sustained EGFR transactivation in rat mesangial cells through non-ligand-dependent pathways.[21] During cancer metastasis, the TGF-β pathway and other signaling cascades, including EGFR/RAS, often cooperate to induce EMT.[22] Wei et al. found that the expression of TGF-β1 and TGF-α was significantly increased in the supernatant of U87-EGFRvIII cells compared with U87 cells by cytokine antibody array analysis.[23] Zhang et al.[24] found that TGF-β2 expression was upregulated in EGFRvIII-positive specimens using tissue staining.

However, no study has been devoted into the production of IGFBP3 in EGFRvIII-expressing cells in immunosuppressive microenvironment, as well as the mechanism underlying action. In this study, we hypothesized that TGF-β and EGFRvIII signaling jointly mediate IGFBP3 production. On the one hand, exogenous TGF-β administration was applied to simulate immunosuppressive microenvironment for the EGFRvIII-overexpressing GBM and-vector cells. The production, transcription factor, and upstream pathways of IGFBP3 expression were investigated. On the other hand, expression of EGFRvIII and the TGF-β-induced malignant progression of EGFRvIII-expressing cells were explored under the treatment of *IGFBP3* siRNA or the addition of IGFBP3 neutralizing antibody. For the first time, we demonstrated that transactivation of TGF-β and EGFRvIII co-activates the Smad2/3 and ERK1/2 signaling pathways and the downstream transcription factor c-Jun, which specifically binds to the promoter region of IGFBP3 and promotes the malignant progression of EGFRvIII-expressing cells. Remarkably, the positive feedback loop of p-EGFRvIII/IGFBP3 under administration of TGF-β was observed. Our findings suggested further clinical trials with the inhibition of IGFBP3 expression in EGFRvIII-expressing GBM.

RESULTS

EGFRvIII and TGF-β synergistically promoted expression of IGFBP3 through Smad2/3 and ERK1/2 signaling pathways

Expression of cytoplasmic (c-) and secretory (s-) IGFBP3 in U87-vector and U87-EGFRvIII cells were assessed. qRT-PCR showed that the expression of IGFBPs in U87-vector cells did not change significantly after TGF-β treatment, whereas in U87-EGFRvIII cells, IGFBP3 increased more significantly after TGF-β treatment (Figure 1A). Western blotting results showed that TGF-β only induced the expression of c-IGFBP3 in EGFRvIII-expressing GBM cells in a time-dependent manner; however, it did not increase over time in vector cells (Figures 1B and S1A). Likewise, the TGF-β induced secretion of s-IGFBP3 in conditioned medium in a time-dependent manner in EGFRvIII-expressing GBM cells, whereas there was no change in secretion of secretory IGFBP3 in vector cells (Figures 1C and S1B). The cell supernatant was further verified by western blotting, and the same experimental results were obtained. To investigate the role of key signaling mediators in the upregulation of IGFBP3, we treated GBM cells with TGF-β at four different time points. The results showed that TGF-β not only elevated phosphorylated canonical Smad2/3 in a time-dependent manner, but also elevated the levels of p-EGFRvIII, p-ERK1/2, and p-AKT in U87-EGFRvIII cells, whereas those proteins in U87-vector cells displayed no significant alterations over time (Figure 1D). Consistent results were obtained for the LN229 clones (Figure S1C). To verify the vital connection between TGF-β and EGFRvIII, U87-EGFRvIII cells were treated with TGF-β and immunoprecipitation was performed. Specifically, the cell lysate was precipitated with anti-IgG, EGFRvIII mAb, followed by immunoblotting with the anti-EGFRvIII and TGF-β mAb. The results showed that positive co-precipitation of EGFRvIII with TGF-β (Figure 1E). Furthermore, to determine the roles of TGF-β, as well as the associated pathways, in EGFRvIII signaling activation and IGFBP3 upregulation, we treated the cells with the TGF-βR inhibitor LY2157299 at different concentrations (0, 5, 10 and 20 μM). The results presented reductions of p-EGFRvIII and IGFBP3 in a dose-dependent manner with reduced expression of p-Smad2/3, p-ERK1/2 and p-AKT (Figure 1F), indicating crucial role of TGF-β and implications of Smad, ERK1/2 and AKT signaling activation in IGFBP3 production. To further explore the role of ERK1/2 and AKT in TGF-β-induced increases in IGFBP3 expression, we pretreated U87-EGFRvIII cells with the MEK inhibitor U0126 and PI3K inhibitor LY294002. As shown in Figure 1G, U0126 and LY294002 significantly reduced the expression levels of p-EGFRvIII and IGFBP3. Together, these data suggested that TGF-β and EGFRvIII synergistically transactivated the Smad2/3 and ERK1/2 signaling pathways, which subsequently upregulated IGFBP3 expression.

TGF-β simultaneously induced nuclear translocation of IGFBP3, EGFRvIII and associated signaling molecules

IGFBP3 is a functional nuclear localization signal, and extensive cell biology studies have suggested important biological roles for IGFBP3 in the nucleus.[25] Immunofluorescence showed that TGF-β treatment

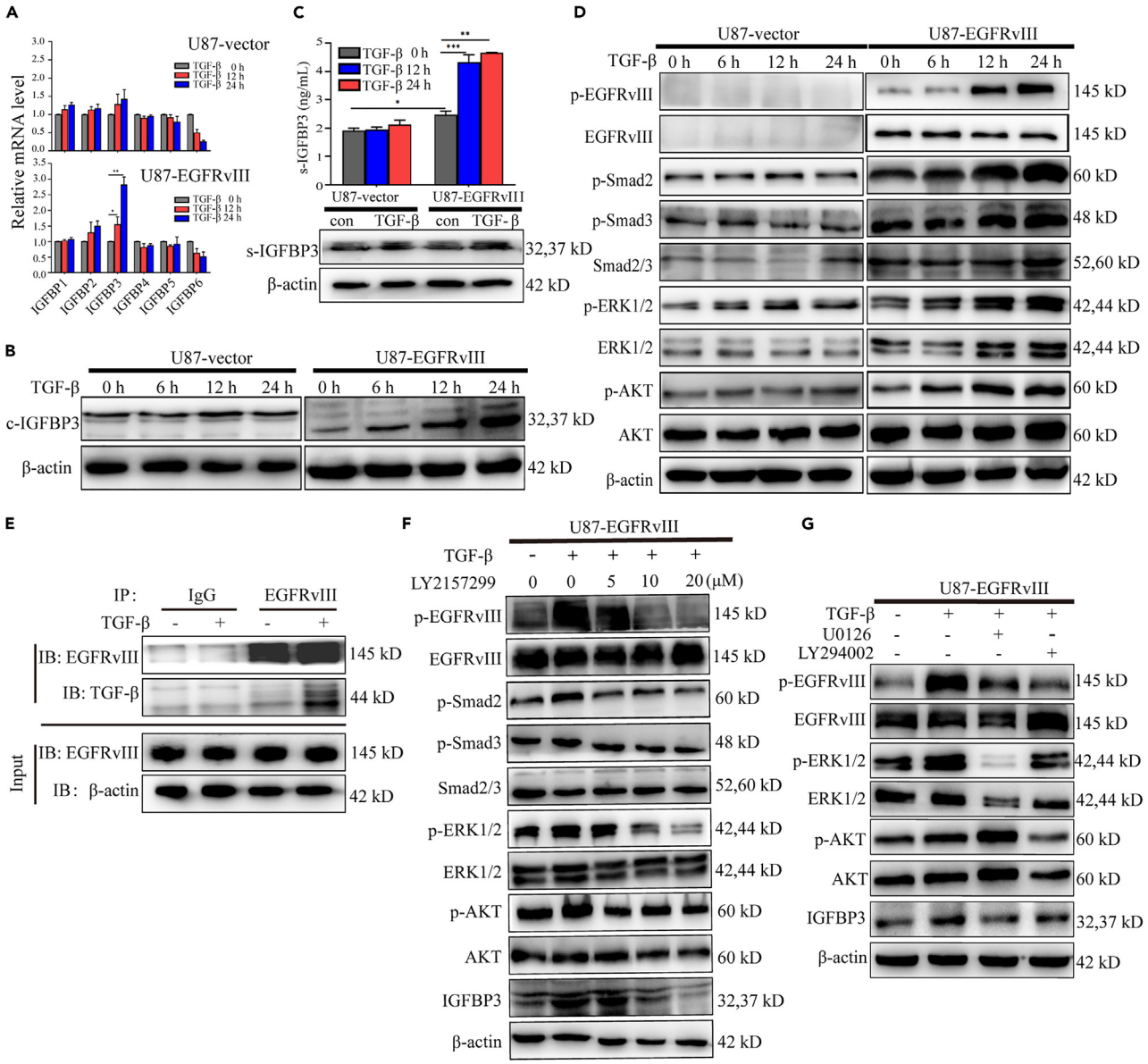

Figure 1. EGFRvIII and TGF-β synergistically promoted expression of IGFBP3

(A) qRT-PCR analysis of *IGFBPs* mRNA in U87-vector and-EGFRvIII with TGF-β (10 ng/mL) treated for 12 h and 24 h.

(B) Western blotting analysis of expression of IGFBP3 in U87-vector and-EGFRvIII cells treated with TGF-β for indicated times, β-actin was used as a loading control.

(C) The expression of IGFBP3 in cell culture supernatant was detected by ELISA and western blotting under TGF-β treatment.

(D) Western blotting analysis of the expression of total and phosphorylation of EGFRvIII, Smad2/3, ERK1/2, AKT in U87-EGFRvIII cells or U87-vector cells treated with TGF-β.

(E) The analysis of immunoprecipitation (IP) showed the firm association of EGFRvIII with TGF-β in U87-EGFRvIII cell.

(F) Western blotting analysis of the expression level of IGFBP3, p-EGFRvIII, and downstream signal proteins in U87-EGFRvIII cells treated with the TGF-βR inhibitor LY2157299 (0, 5, 10 and 20 μM) and then stimulated with TGF-β. (G) Protein expression levels of total and phosphorylated of EGFRvIII, ERK1/2, AKT and IGFBP3 in U87-EGFRvIII cells pretreated with U0126 (15 μM) or LY294002 (15 μM) and then stimulated cells with TGF-β. Values are the means ± SD of three independent experiments. *p<0.05; **p<0.01; ***p<0.001. See also Figure S1.

simultaneously induced nuclear translocation of IGFBP3 and EGFRvIII (Figure 2A). Subsequently, nuclear proteins were isolated to verify the expression of EGFRvIII and related signaling molecules, indicating an increasing trend of p-EGFRvIII, p-Smad2/3 and p-ERK1/2 along with increasing c-IGFBP3 expression under TGF-β treatment (Figure 2B). Similar results were obtained for LN229-EGFRvIII cells after the

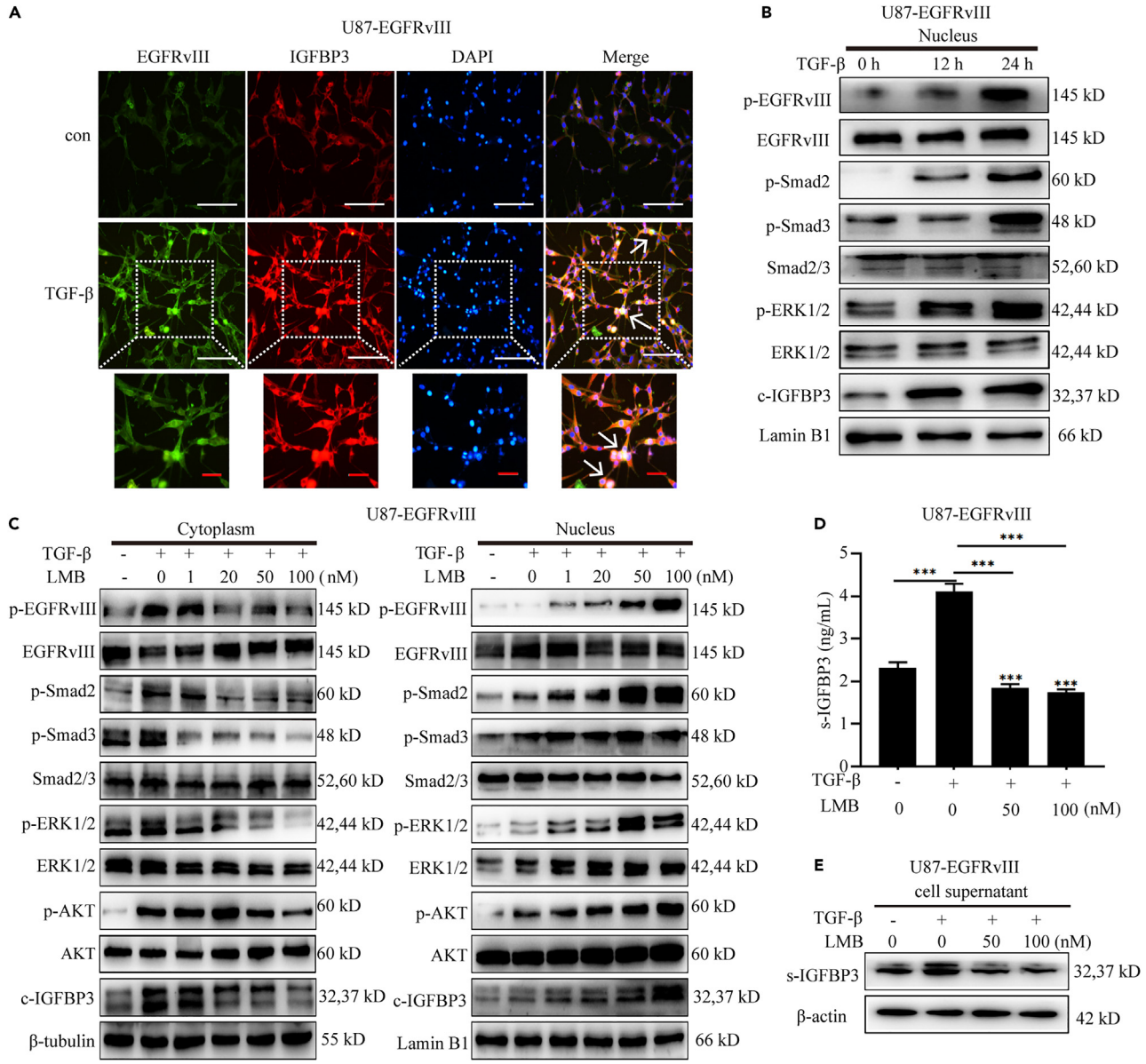

Figure 2. TGF-β induced IGFBP3 and EGFRvIII nuclear translocation

(A)Immunofluorescence staining of EGFRvIII (green), IGFBP3 (red) and DAPI (blue) in U87-EGFRvIII cells after TGF-β treatment. Scale bar = 25 μm, arrows showed changes in the co-localization of EGFRvIII and IGFBP3.

(B) Western blotting analysis of the nuclear protein levels of IGFBP3, total and phosphorylated of EGFRvIII, Smad2/3 and ERK1/2 after TGF-β treatment.

(C) The expression level of IGFBP3, TGF-β and EGFRvIII downstream signal proteins were detected in the nuclear and cytoplasmic of U87-EGFRvIII cells treated with LMB and then stimulated with TGF-β.

(D) ELISA analysis of the expression level of secreted IGFBP3 in U87-EGFRvIII cell culture supernatant pretreated with LMB and then stimulated with TGF-β.

(E) The protein expression level of IGFBP3 in cell supernatant of U87-EGFRvIII cells pretreated with LMB and then stimulated with TGF-β. ***p<0.001. See also Figure S2.

same treatment (Figure S2A). Moreover, nuclear export inhibitor leptomycin B (LMB) significantly elevated levels of p-EGFRvIII, p-Smad2/3, p-ERK1/2, p-AKT and c-IGFBP3 in the nucleus but reduced their protein levels in the cytoplasm of EGFRvIII-expressing GBM cells in a dose-dependent manner (Figures 2C and S2B). Therefore, our findings indicated co-nuclear translocation of IGFBP3 and EGFRvIII induced by TGF-β. Meanwhile, ELISA detected that s-IGFBP3 in the cell supernatant were reduced with increased concentration of LMB (Figures 2D and S2C), which was further confirmed by western blotting (Figure 2E).

Activated by TGF-β and EGFRvIII signals, transcription factor c-Jun can bind to the IGFBP3 promoter region

The proto-oncogene c-Jun is a major component of the heterodimeric AP-1 family of transcription factors. c-Jun has been reported to be a downstream target of ERK1/2.[26] Meanwhile, another study[27] proposed that TGF-β regulates cell migration through endogenous c-Jun; however, the relationship between c-Jun activation and IGFBP3 production has not been reported. Considering that IGFBP3 expression was regulated by the TGF-β signaling pathway, we speculated that c-Jun might play a key role in TGF-β-mediated upregulation of IGFBP3. To further investigate the potential mechanisms, the roles of c-Jun in TGF-β-mediated upregulation of IGFBP3 were explored. As shown in Figures 3A and 3B, the mRNA and protein expression levels of c-Jun were significantly increased in U87-EGFRvIII cells rather than U87-vector cells after they were exposed to TGF-β for 24 h. The c-Jun protein levels were also verified in LN229-EGFRvIII and LN229-vector cells (Figure S3A). In addition, LY2157299, U0126 and LY294002 were applied to examine the roles of TGF-βR, ERK1/2 and AKT signaling in c-Jun expression (Figures 3C and 3D), demonstrating attenuated c-Jun expression as same as expression of IGFBP3.

To determine whether c-Jun binds to the IGFBP3 promoter to activate it, we used online bioinformatics tools to analyze the IGFBP3 promoter region. As shown in Figure 3E, the putative binding sites of highest score for transcription factor c-Jun were −742 to −732 relative to the transcription initiation site. Moreover, the c-Jun binding sites on IGFBP3 conserved sequences were mutated. Next, a panel of firefly luciferase reporter plasmids containing the IGFBP3 promoter region was examined using transient transfection assays. pcDNA3.1 (+) with a c-Jun conserved sequence was co-transfected with the GPL3-IGFBP3-WT or GPL3-IGFBP3-Mut plasmid. As shown in Figure 3F, c-Jun specifically bound to the WT-IGFBP3 promoter, but not to the Mut-IGFBP3 promoter. To confirm the effect of c-Jun on TGF-β induced IGFBP3 expression, *c-Jun* siRNA was applied. As shown in Figures 3G and 3H, *c-Jun* siRNA effectively reversed TGF-β-induced c-Jun elevation compared to the negative control in U87-EGFRvIII cells. At the same time, IGFBP3 expression was significantly impaired with the impaired c-Jun expression, demonstrating that c-Jun was the transcription factor of IGFBP3. Moreover, our results also observed that expression of p-EGFRvIII was impaired (Figure 3H).

IGFBP3 play important roles in enhanced malignant behaviors of EGFRvIII-expressing GBM cells under TGF-β stimulation

Because exogenous TGF-β induced EGFRvIII-positive GBM cells to express IGFBP3, the malignant biological behavior of cells was compared between -EGFRvIII and -vector cells to examine whether EGFRvIII-positive cells acquire stronger malignant characteristics. The proliferation ability of U87-vector cells was slightly enhanced after 48 h of TGF-β treatment, whereas the proliferation of U87-EGFRvIII cells was significantly elevated (Figure 4A). These data were confirmed in LN229 clones (Figure S4A) as well. Consistently, cell cycle analysis showed that the growth ratio of S-phase cells in the U87-vector cells after 48 h of TGF-β treatment was about 9%, in comparison with around 16% of that in U87-EGFRvIII cells (Figure 4B). Western blotting showed that the expression levels of S-phase related protein (Cyclin E1, Cyclin E2 and CDK2) were significantly increased in U87-EGFRvIII cells after TGF-β treatment (Figure 4C). Meanwhile, wound healing and transwell invasion assays demonstrated that the migration and invasion rates of U87-EGFRvIII cells were significantly increased compared with U87-vector cells (Figures 4D and 4E). Likewise, the migration ability of LN229-EGFRvIII cells stimulated with TGF-β was significantly strengthened than that of LN229-vector cells (Figure S4B). Moreover, the EMT markers (*e.g.*, N-cadherin, Snail and Desmoplakin) of U87-EGFRvIII and U87-vector cells were detected after treatment with TGF-β. Although the results showed changes in U87-vector cells, its reactivity was significantly lower than that for U87-EGFRvIII cells (Figure S4C). This was further confirmed by western blotting analysis of N-cadherin, E-cadherin and Vimentin expression levels (Figure S4D).

To investigate whether IGFBP3 plays a vital role in malignant biological behavior of EGFRvIII-positive cells under the administration of exogenous TGF-β, we knocked down *IGFBP3* expression using siRNA. Western blotting and qRT-PCR verified that *IGFBP3* siRNA significantly reduced the expression of IGFBP3 in both U87-EGFRvIII and U87-vector, particularly, *IGFBP3* siRNA partially counteracted TGF-β-induced IGFBP3 elevation in U87-EGFRvIII cells (Figures 5A and S5A). Similar results were obtained in the LN229 clones (Figure S5B). Significantly, *IGFBP3* siRNA also significantly reduced the expression of s-IGFBP3 in the cell culture supernatant, as determined by ELISA (Figures S5C, S5D). *IGFBP3* siRNA was used to detect its impact on the malignant biological behavior of EGFRvIII-expressing cells under the administration of exogenous TGF-β. Flow cytometry indicated that *IGFBP3* siRNA reduced the proportion of cells at S-phase compared

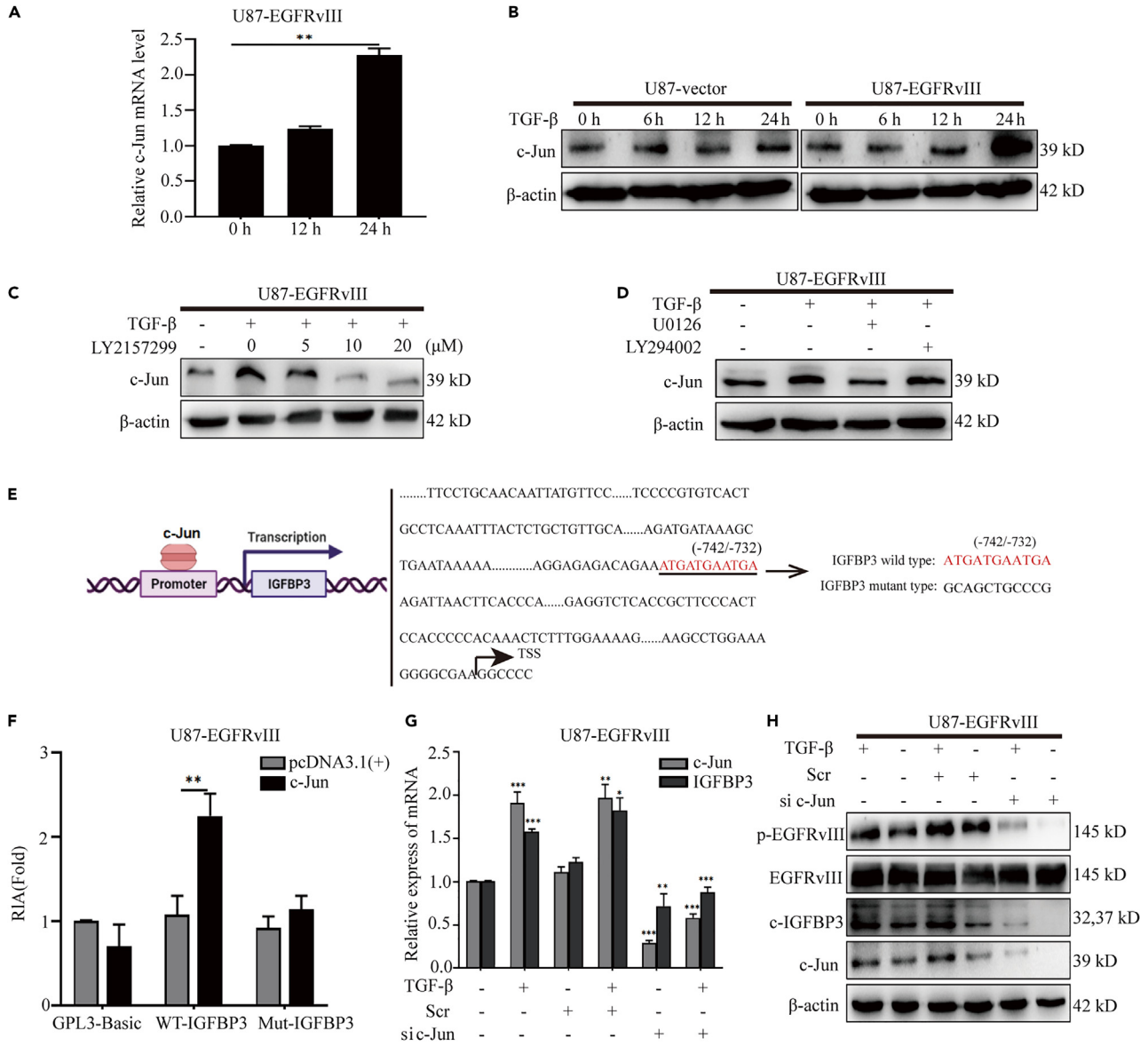

Figure 3. TGF-β regulates the transcription of IGFBP3 by activating the transcription factor c-Jun

(A) The mRNA of *c-Jun* was detected in U87-EGFRvIII by qRT-PCR after TGF-β treatment.

(B) Western blotting analysis of c-Jun protein levels in U87-vector or U87-EGFRvIII cells treated with TGF-β for indicated times.

(C) Western blotting analysis of the expression level of c-Jun in U87-EGFRvIII cells treated with LY2157299 (0, 5, 10 and 20 μM) and then stimulated with TGF-β.

(D) Protein expression levels of c-Jun in U87-EGFRvIII cells pretreated with U0126 and LY294002 and then stimulated cells with TGF-β.

(E) Schematic diagram depicting the regulatory sequences of the IGFBP3 promoter region.

(F) Luciferase assays for specific binding of IGFBP3 promoter (WT) or (mutant)-Luc plasmid to c-Jun plasmid transfected with U87-EGFRvIII.

(G) U87-EGFRvIII cells were transfected with Scramble (Scr) or *c-Jun* specific siRNA, then treated with TGF-β for 24 h, the expression level of *c-Jun* and *IGFBP3* mRNA were determined by qRT-PCR analysis.

(H) Western blotting analysis of the effect of *c-Jun* knockdown on TGF-β-induced upregulation of c-Jun, IGFBP3 and EGFRvIII proteins level. *p<0.05; **p<0.01; ***p < 0.001. See also Figure S3.

to the negative control group or TGF-β-treated group alone (Figure 5B). Then, the proteins expression of Cyclin E1, Cyclin E2 and CDK2 related to S-phase was tested by western blotting in these cells and obtained the same results (Figure 5C). Assays of wound healing and transwell demonstrated that IGFBP3 significantly impaired the TGF-β-induced enhancement of migration and invasion capabilities in U87-EGFRvIII cells

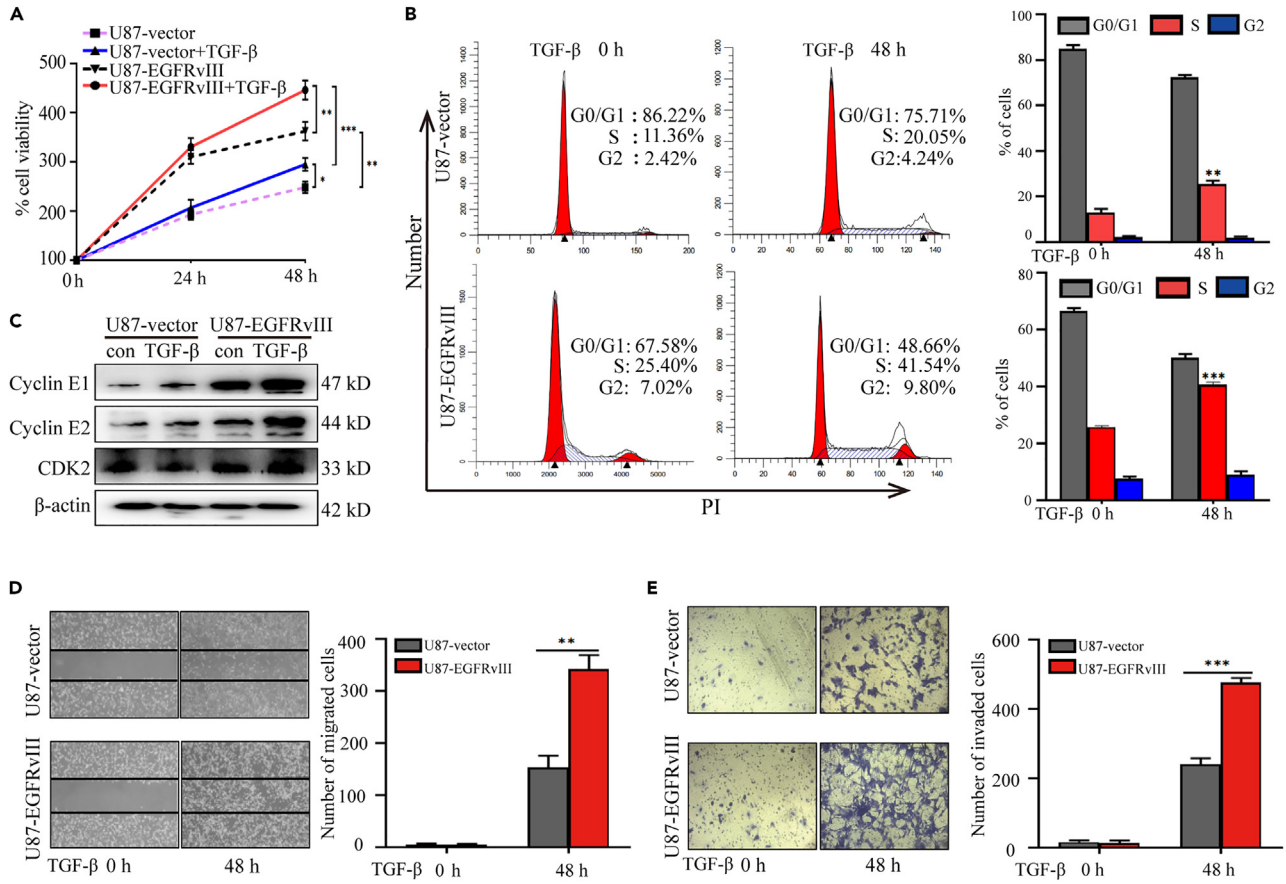

Figure 4. The malignant biological behavior of EGFRvIII-expressing GBM cells was regulated by TGF-β

(A) MTT assay was performed to analyze the cell proliferation between U87-vector cells and U87-EGFRvIII cells under the treatment of TGF-β for 48 h.

(B) DNA content of U87-vector and U87-EGFRvIII cells was assayed by flow cytometry and PI staining. The gates and percentages of cells in the G1, S, and G2 phases are indicated.

(C) Western blotting analysis the effects of TGF-β on S-phase related proteins (Cyclin E1, Cyclin E2 and CDK2) in U87-vector and U87-EGFRvIII cells.

(D and E) U87-vector and U87-EGFRvIII cells were wound healing and transwell invasion assays treated to measure and quantify their migration and invasion activity under the treatment of TGF-β. *p<0.05; **p<0.01; ***p<0.001. See also Figure S4.

(Figure 5D). Moreover, the effects of *IGFBP3* knockdown on the Smad2/3, ERK1/2, AKT, MMP2 and MMP9 were examined by western blotting. As shown in Figures 5E and S5E, knockdown of *IGFBP3* resulted in decreased p-EGFRvIII and p-Smad2/3, in addition to greatly reduced phosphorylation of ERK1/2 and AKT in EGFRvIII-expressing GBM cells. In contrast, these molecules were less inhibited in the vector cells. At the same time, *IGFBP3* siRNA reversed the TGF-β and EGFRvIII induced increase of MMP-9 and MMP-2 (Figure 5E). The above findings suggested a feedback loop of TGF-β/EGFRvIII and IGFBP3. Therefore, IGFBP3 neutralizing antibody (IGFBP3-Ab) at different concentrations was subsequently added to conditioned medium of U87-EGFRvIII to confirm the potential effect of s-IGFBP3 on TGF-β and EGFRvIII signaling. As shown in Figure 5F, IGFBP3-Ab significantly inhibited the TGF-β-induced invasion ability of the U87-EGFRvIII cells. Western blotting presented consistent results with those after knockdown of *IGFBP3*, that is, decreased expression of p-EGFRvIII, p-Smad2, and p-Akt (Figure 5G). These results indicate that inhibition of IGFBP3 could reverse TGF-β-induced malignant biological behavior in EGFRvIII cells.

Mouse model and clinical investigations suggested IGFBP3 as an effective therapeutic target

Subcutaneous xenograft mouse models were established to validate the effects of IGFBP3 on tumor growth *in vivo*. The mouse subcutaneous xenograft models were generated using *IGFBP3* knockdown or negative control U87-EGFRvIII cells. As the results, *IGFBP3* knockdown presented delayed tumor growth (Figure 6A) and decreased tumor weight (Figure 6B). To further verify the effect of *IGFBP3* knockdown on the survival of mice, the constructed U87-EGFRvIII-shControl and U87-EGFRvIII-shIGFBP3 cells were injected into the

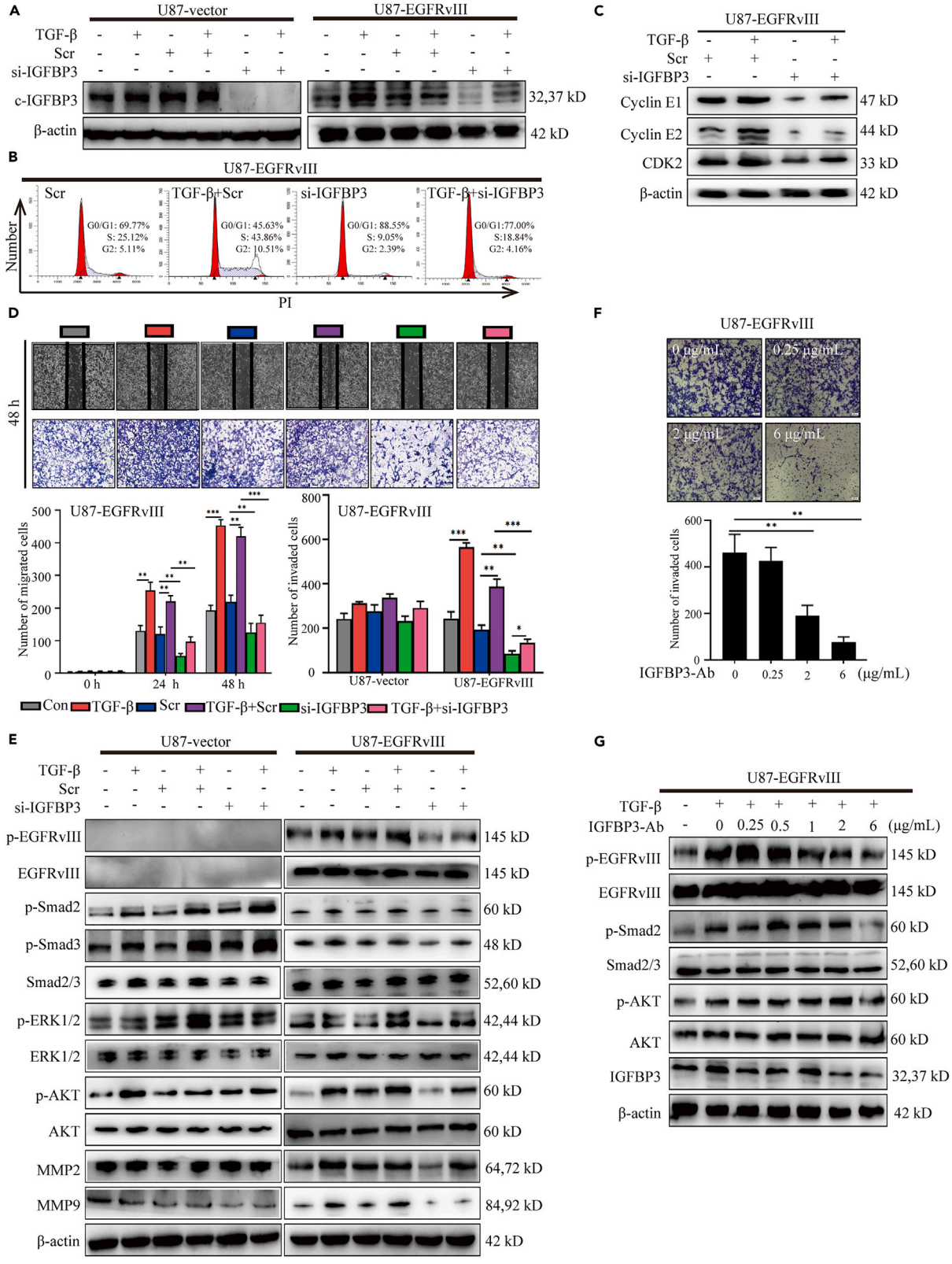
A
U87-vector
U87-EGFRvIII
TGF-β
Scr
si-IGFBP3
c-IGFBP3
β-actin
32,37 kD
42 kD
B
U87-EGFRvIII
Scr
TGF-β+Scr
si-IGFBP3
TGF-β+si-IGFBP3
G0/G1: 69.77%
S: 25.12%
G2: 5.11%
G0/G1: 45.63%
S: 43.86%
G2: 10.51%
G0/G1: 88.55%
S: 9.05%
G2: 2.39%
G0/G1:77.00%
S:18.84%
G2: 4.16%
Number
PI
C
U87-EGFRvIII
Cyclin E1
Cyclin E2
CDK2
47 kD
44 kD
33 kD
D
48 h
U87-EGFRvIII
Number of migrated cells
0 h
24 h
48 h
Number of invaded cells
U87-vector
Con
TGF-β
Scr
TGF-β+Scr
si-IGFBP3
TGF-β+si-IGFBP3
E
p-EGFRvIII
EGFRvIII
p-Smad2
p-Smad3
Smad2/3
p-ERK1/2
ERK1/2
p-AKT
AKT
MMP2
MMP9
145 kD
60 kD
48 kD
52,60 kD
42,44 kD
64,72 kD
84,92 kD
F
0 μg/mL
0.25 μg/mL
2 μg/mL
6 μg/mL
IGFBP3-Ab
(μg/mL)
G
IGFBP3

Figure 5. IGFBP3 enhanced the malignant behavior of EGFRvIII-expressing cells under the administration of exogenous TGF-β

(A) U87-vector and U87-EGFRvIII cells were transfected with Scr or *IGFBP3* specific siRNA, and the expression level of *IGFBP3* protein were determined by western blotting.

(B) Effect of IGFBP3 knockdown on cell cycle distribution under the treatment of TGF-β.

(C) Western blotting analysis the effect of *IGFBP3* knockdown on S-phase related protein expression under the treatment of TGF-β.

(D) Knockdown of *IGFBP3* decreases the migration and invasion capacities induced by TGF-β in U87-EGFRvIII cell, quantitative images of migrant and invasive cells were shown based on wound healing and transwell assay.

(E) Western blotting analysis of the effect of *IGFBP3* knockdown on TGF-β-induced upregulation of p-EGFRvIII, p-Smad2/3, p-ERK1/2, p-AKT and MMP2/9 proteins level in U87-EGFRvIII cell and U87-vector cell.

(F) Anti-IGFBP3 decreases the invasion capacities induced by TGF-β.

(G) Western blotting analysis of the effect of anti-IGFBP3 on TGF-β-induced upregulation of p-EGFRvIII, p-Smad2 and p-AKT proteins level in U87-EGFRvIII cell. *p<0.05; **p<0.01; ***p<0.001. See also Figure S5.

intracranial of mice, and the results showed that IGFBP3-shRNA-treated mice showed better overall survival compared with shControl-treated mice (Figure 6C). Compared with negative control group, immunohistochemistry showed significantly decreased expression of IGFBP3 along with downregulated expression of tumor tissue proliferation marker Ki-67, and blood vessels marker CD31 in tumor tissue in *IGFBP3* knockdown group (Figure 6D). These results indicated that IGFBP3 knockdown significantly suppressed tumor growth and tumor formation *in vivo*. In addition, a series of human biopsies, including that of normal tissues (n = 3) and patients with newly diagnosed grades I-II (n = 12), III (n = 23), and IV (GBM) (n = 42) glioma were examined to further explore whether the expression of EGFRvIII and IGFBP3 has a synergistic promoting effect on patients with glioma. IHC analysis showed that IGFBP3 and EGFRvIII were highly expressed in GBM compared to that in patients with normal tissue or low-grade glioma (Figures 7A and 7B). Moreover, correlation analysis of the 42 GBM specimens showed that expression level of EGFRvIII was positively correlated with that of IGFBP3 (Figure 7C).

DISCUSSION

A conceptual model of the feedback loop between p-EGFRvIII and IGFBP3 in EGFRvIII-expressing GBM cells under administration of TGF-β

Although that the expression of EGFRvIII was restricted on tumors cells has made EGFRvIII an ideal target for GBM in theory, the immunosuppressive microenvironment has been recognized as key constraint of EGFRvIII targeting therapy. TGF-β is an important component of the GBM microenvironment that inhibits the immune response and promotes the occurrence and development of glioma by affecting the gene expression profile of glioma cells.[28] Several studies have demonstrated the associations between TGF-β and EGFR and between TGF-β2 and EGFRvIII, as well as their important roles, in the progression of GBM.[21–24] However, few studies illustrating the associations between TGF-β and EGFRvIII have been reported in GBM. In this study, we demonstrated that TGF-β promoted the proliferation and invasion of EGFRvIII-expressing GBM cells more significantly than the vector cells (Figure 4). Studies have shown that the G1 to S phase (G1/S) transition was the key step that driving cells into the division cycle and was regulated by cell cycle regulatory proteins, such as CDK2, cyclin E and p53.[29,30] Our results found that the proportion of S-phase in U87-EGFRvIII cells was obvious increased compared with U87-vector cells, and the proportion increased more significantly when TGF-β was added to U87-EGFRvIII cells. Meanwhile, the cross talk between TGF-β and EGFRvIII signaling, which could be agreed by the cross talk between TGF-β and EGFR,[31,32] was observed in this study. In osteosarcoma cells, TGF-β indirectly activates the Ras/Raf/MAPK pathway and induces the expression IGFBP3; however, the origin of IGFBP3 in GBM has not been reported. In this study, c-IGFBP3 was detected in U87-vector cells but not showed associations with TGF-β (Figure 1B). In contrast, TGF-β could promote expression of c-IGFBP3 in a dose-dependent manner when EGFRvIII expressed, indicating crucial roles of the cross talk between TGF-β and EGFRvIII signaling in producing IGFBP3. In addition, IGFBP3 is a functional nuclear localization signal, and extensive cell biology studies have suggested important biological roles for IGFBP3 in the nucleus.[25] Cellular uptake and nuclear import of IGFBP3 have been extensively studied.[25,33] Here, immunofluorescence and nuclear protein isolation showed that TGF-β induced the nuclear translocation of IGFBP3 and EGFRvIII.

At present, transcription factors of IGFBP3 have been reported, including X-box binding protein 1 (XBP1)[34] and homeobox D10 (HoxD10).[35] Deivendran et al.[36] proposed that c-Jun acts as a cofactor for IGFBP3 transcription in breast cancer. In this study, the inhibition of the ERK1/2 and AKT pathway by using the inhibitor U0126 and LY294002 could attenuate the TGF-β-induced c-Jun upregulation. For the first time, we reported that c-Jun directly binds to the IGFBP3 promoter to activate the expression of IGFBP3 in

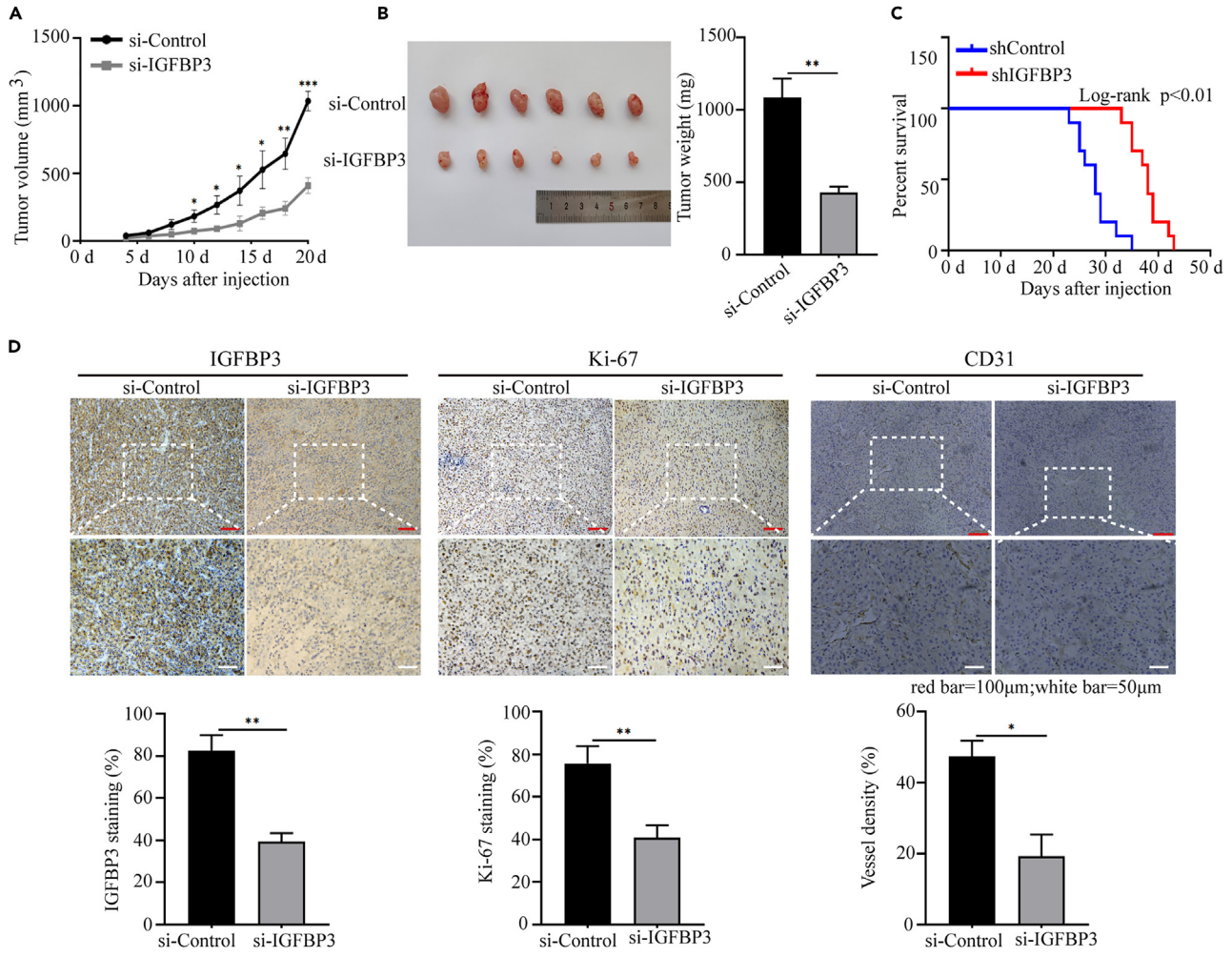

Figure 6. Effect of *IGFBP3* knockdown *in vivo* growth of U87-EGFRvIII cells using mice subcutaneous xenograft models. Nude mice were subcutaneously injected with pretreated U87-EGFRvIII-*siIGFBP3* and U87-EGFRvIII-*siControl* cells (n = 5 for each group)

(A) Tumor growth curves show tumor size measured every two days.

(B) Tumor images and weights of the removed subcutaneous tumors after inoculation for 21 days.

(C) The overall survival of mice in the U87-EGFRvIII-shControl and U87-EGFRvIII-shIGFBP3 cells implanted groups. Median survival of each group was 28 days for shControl, 38 days for shIGFBP3. n = 10, **p < 0.01 compared to the control, logrank test.

(D) Representative images of IGFBP3, Ki-67 and tumor angiogenesis stained with CD31 in mouse subcutaneous tumors by IHC. *p < 0.05; **p < 0.01; ***p < 0.001.

EGFRvIII-expressing GBM cells, and that knockdown of *c-Jun* in EGFRvIII GBM cells also decreases the up-regulated IGFBP3 expression induced by TGF-β treatment.

Remarkably, our findings demonstrated a positive feedback loop of p-EGFRvIII/c-IGFBP3/s-IGFBP3/p-EGFRvIII (Figure 8), which greatly contributed to the enhanced malignant behaviors of EGFRvIII-expressing GBM cells under administration of TGF-β. Our results showed that TGF-β could also induce the elevation of s-IGFBP3 in cell supernatants of EGFRvIII-expressing cells. Research has found that patients with high levels of IGFBP3 in plasma had shorter overall survival in GBM,[37] which can be combined with our results and suggested that plasma IGFBP3 might be a potential biomarker for predicting GBM progression. IGFBP3 has been proposed as a functional ligand for the serine/threonine kinase type V transforming growth factor β receptor (TGF-βRV).[38] Martin et al.[39] found that IGFBP3 stimulated the growth of breast epithelial cells by increasing EGFR phosphorylation and MAPK signaling. In this study, downregulation of IGFBP3 attenuated the malignant biological behavior of U87-EGFRvIII cells induced by TGF-β. Mechanistically, *IGFBP3* siRNA or neutralizing antibodies significantly attenuated the activation of the TGF-β and

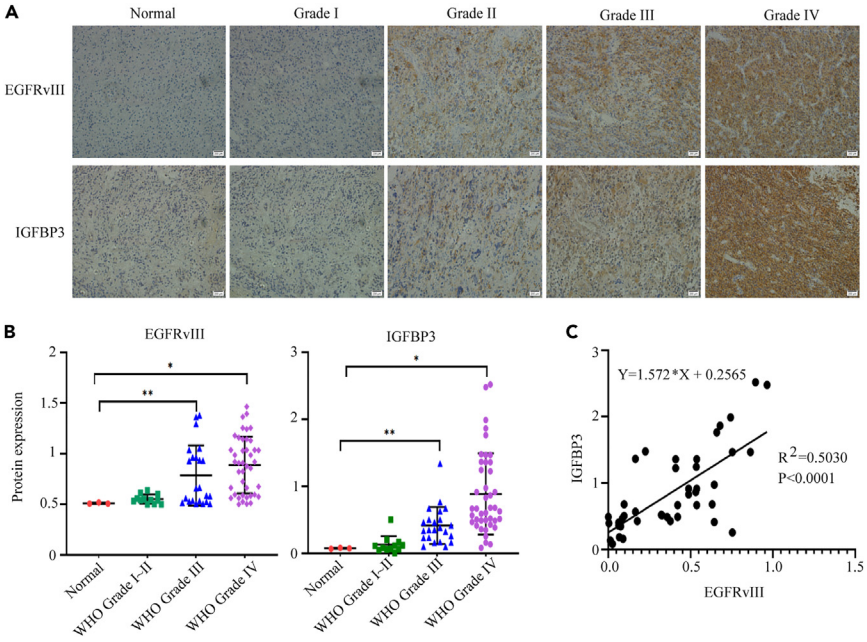

Figure 7. EGFRvIII and IGFBP3 expression levels in glioma tissues

(A) Representative IHC stained images of glioma tissues using the anti-EGFRvIII and anti-IGFBP3 antibodies.

(B) EGFRvIII and IGFBP3 protein expression in tissue specimens from Normal tissue and WHO I ∼ IV glioma patients.

(C) Correlation analysis of EGFRvIII and IGFBP3 in tissues. *p < 0.05; **p < 0.01.

EGFRvIII signaling pathways, including downstream activation of Smad, ERK1/2, AKT, and MMP2/9, whereas these results were not observed in vector cells. These data implied that TGF-β and EGFRvIII mediate IGFBP3 production and together form a loop between them to influence GBM progression.

IGFBP3 may serve as an additional target in EGFRvIII targeting therapy

IGFBPs are a series of cystine-rich proteins that play important roles in tumor occurrence and development.[40] Among IGFBPs, the expression level of isoforms-2, -3, and -5 have been investigated extensively in gliomas. IGFBP3 can act as a tumor suppressor and promoter in a tissue-specific manner. A wealth of evidence has revealed both tumor suppressing and tumor promoting effects of IGFBP3 depending on cell types, post-translational modifications and cellular context.[7] Studies have demonstrated IGFBP3 has often been considered as a tumor suppressor against the prostate cancer, esophageal squamous cell carcinoma.[41,42] However, IGFBP3 functions as a tumor promoter in some cancers, including breast cancer and melanoma.[10,43] Santosh et al.[15] reported that IGFBP3 emerges as a strong predictor of survival in patients with newly diagnosed glioblastoma. Our results confirm that IGFBP3 promotes malignant progression of EGFRvIII-expressing GBM.

The tumor microenvironment plays a critical role in GBM development, progression, and prognosis. Recently, many studies using single cell transcriptomics have demonstrated the tumor microenvironment could modulate GBM cellular states with notable plasticity, challenging the long-term assumption that GBM tumors were clonal masses with the same molecular characteristics.[2,44] Single-Cell Atlas has identified the initial and recurrent GBMs sharing similar suppressive changes, and among this GBM patients some markers demonstrated different expression levels, including TGF-β.[45] Microarray expression analysis showed that the expression of genes related to TGF-β pathway was increased after serum treatment in primary glioma patients, and TGF-β was sufficient to induce cell senescence, indicating that primary glioblastoma cells retain functional senescence program induced by acute activation of TGF-β signaling pathway.[46] Studies have showed that the proliferation effect of TGF-β on different glioma cell lines is different, partly because of the expression levels of TGF-β receptor and Smad, in addition, the imbalance between Smad and MAPK pathways is responsible for TGF-β carcinogenesis.[47,48] In this study, we for the first time

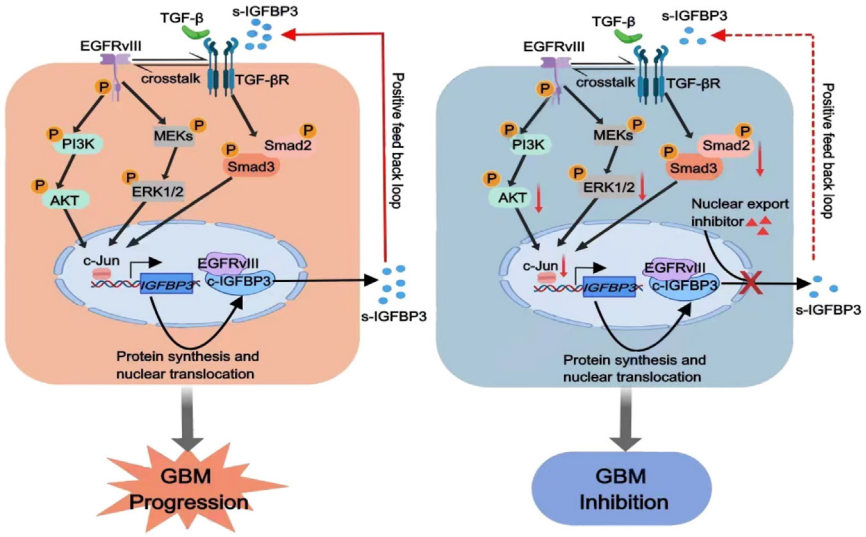

Figure 8. Schematics illustration depicting the key findings of this study

TGF-β and EGFRvIII transactivation induced the positive feedback loop of IGFBP3 to promote the progression of EGFRVII-positive GBMs, and targeted IGFBP3 can correct this vicious cycle to combat EGFRvIII-positive GBMs.

demonstrated that inhibition of IGFBP3 could reverse TGF-β-induced malignant biological behavior in EGFRvIII cells, probably via impairing the expression of p-EGFRvIII, p-Smad2, p-ERK1/2 and p-Akt (Figure 5).

In addition, genetic polymorphisms and haplotypes within the EGFR and IGFBP3 genes are associated with an increased risk of renal cancer.[49] IGFBP3 and EGFR form complexes in the nucleus of breast cancer cells that mediates resistance to DNA-damaging drugs, suggesting that they may be involved in the regulation of DNA repair.[50] Increased expression of IGFBP3 was detected in lung adenocarcinomas with EGFR mutations that developed resistance mechanisms after prolonged exposure to increased doses of afatinib.[51] TGF-β1, EGF and IGFBP-3 genes were most upregulated in breast cancer cells after long-term trastuzumab (monoclonal antibody targeting HER2) exposure, and these genes play a key role in trastuzumab resistance.[52] Recent reports have indicated targeting EGFR signaling alone has been of little success in triple-negative breast cancer (TNBC) which frequent expression of IGFBP3 and EGFR highly. The interaction between EGFR and IGFBP3 may also promote chemoresistance and inhibition of both has shown promise in a preclinical setting in TNBC.[16] To the best of our knowledge, we are the first to report that down-regulating IGFBP3 impairs EGFRvIII signaling activation in EGFRvIII-expressing GBM cells. Additionally, we further verified that targeted IGFBP3 therapy effectively disrupted the EGFRvIII-induced network in GBM by effective gene knockdown assays for IGFBP3 *in vivo* and *in vitro*.

In conclusion, our study demonstrated that IGFBP3 production was mediated through the TGF-β/EGFRvIII/c-Jun axis. Inhibition of IGFBP3 significantly reduced the malignant behavior induced by TGF-β in EGFRvIII-expressing cells but not in vector cells. Hence, understanding the mechanism of IGFBP3 involved in growth stimulatory signal transduction, and to design a combined therapy may improve the efficacy of GBM in which EGFRvIII and IGFBP3 overexpression.

Limitations of the study

In this study, although treatment with *IGFBP3* knockdown assays significantly decreased cell malignant behavior, this decrease was only validated in two EGFRvIII-expressing human GBM cell lines. Owing to the heterogeneity of GBM tumors, it is unclear whether targeting IGFBP3 is effective on other type EGFRvIII-expressing GBM cells. Furthermore, patient-derived GBM cells with endogenous overexpressed EGFRvIII[53,54] are also needed to be established and tested. In addition, supplementation with exogenous TGF-β did not fully simulate the diverse microenvironments *in vivo*. Further study will be required to better characterize this function.

STAR★METHODS

Detailed methods are provided in the online version of this paper and include the following:

SUPPLEMENTAL INFORMATION

Supplemental information can be found online at https://doi.org/10.1016/j.isci.2023.106639.

ACKNOWLEDGMENTS

We thank Dr. F Furnari (Ludwig Institute for Cancer Research, San Diego, California) for kindly providing the PSK plasmids. This work was supported by the Shandong Provincial Natural Science Foundation of China (ZR2021MH036 to Y.C.D.); the National Natural Science Foundation of China (81402054 to Y.C.D., 61902094 to X.Z., 81472367 to H.R.); the Science and Technology Program of Binzhou Medical University (50012304325 to Y.C.D.).

AUTHOR CONTRIBUTIONS

X.H.Z. and G.Y.W. analyzed and interpreted the experiments and wrote the manuscript. Y.J.G. designed and analyzed the experiments. P.S., H.Z. and L.L.Z. performed immunohistochemistry analysis and the subcutaneous model *in vivo* assays. H.Y.J., Y.R.Z., X.Y.W., and B.W. performed the cell culture and cell behavior experiments. H.R. and X.Z. assisted with data analysis and manuscript preparation. Y.C.D. led the study, supervised the overall project and reviewed the manuscript. All authors read and approved the final manuscript.

DECLARATION OF INTERESTS

The authors declare no competing interests.

Received: November 17, 2022
Revised: March 9, 2023
Accepted: April 5, 2023
Published: April 10, 2023

REFERENCES

1. Wang, Z., Guo, X., Gao, L., Wang, Y., Ma, W., and Xing, B. (2020). Glioblastoma cell differentiation trajectory predicts the immunotherapy response and overall survival of patients. Aging (Albany NY) *12*, 18297–18321. https://doi.org/10.18632/aging.103695.

2. Patel, A.P., Tirosh, I., Trombetta, J.J., Shalek, A.K., Gillespie, S.M., Wakimoto, H., Cahill, D.P., Nahed, B.V., Curry, W.T., Martuza, R.L., et al. (2014). Single-cell RNA-seq highlights intratumoral heterogeneity in primary glioblastoma. Science *344*, 1396–1401. https://doi.org/10.1126/science.1254257.

3. Zong, H., Verhaak, R.G.W., and Canoll, P. (2012). The cellular origin for malignant glioma and prospects for clinical advancements. Expert Rev. Mol. Diagn. *12*, 383–394. https://doi.org/10.1586/erm.12.30.

4. Shergalis, A., Bankhead, A., 3rd, Luesakul, U., Muangsin, N., and Neamati, N. (2018). Current challenges and opportunities in treating glioblastoma. Pharmacol. Rev. *70*, 412–445. https://doi.org/10.1124/pr.117.014944.

5. Verhaak, R.G.W., Hoadley, K.A., Purdom, E., Wang, V., Qi, Y., Wilkerson, M.D., Miller, C.R., Ding, L., Golub, T., Mesirov, J.P., et al. (2010). Integrated genomic analysis identifies clinically relevant subtypes of glioblastoma characterized by abnormalities in PDGFRA, IDH1, EGFR, and NF1. Cancer Cell *17*, 98–110. https://doi.org/10.1016/j.ccr.2009.12.020.

6. Yang, J., Yan, J., and Liu, B. (2017). Targeting EGFRvIII for glioblastoma multiforme. Cancer Lett. *403*, 224–230. https://doi.org/10.1016/j.canlet.2017.06.024.

7. Mao, H., Lebrun, D.G., Yang, J., Zhu, V.F., and Li, M. (2012). Deregulated signaling pathways in glioblastoma multiforme: molecular mechanisms and therapeutic targets. Cancer Invest. *30*, 48–56. https://doi.org/10.3109/07357907.2011.630050.

8. Huang, S., Song, Z., Zhang, T., He, X., Huang, K., Zhang, Q., Shen, J., and Pan, J. (2020). Identification of immune cell infiltration and immune-related genes in the tumor microenvironment of glioblastomas. Front. Immunol. *11*, 585034. https://doi.org/10.3389/fimmu.2020.585034.

9. Cai, Q., Dozmorov, M., and Oh, Y. (2020). IGFBP-3/IGFBP-3 receptor system as an anti-tumor and anti-metastatic signaling in cancer. Cells *9*, 1261. https://doi.org/10.3390/cells9051261.

10. Luo, J., Zhu, H., Chang, H.M., Lin, Y.M., Yang, J., and Leung, P.C.K. (2020). The regulation of IGFBP3 by BMP2 has a role in human endometrial remodeling. Faseb. J. *34*, 15462–15479. https://doi.org/10.1096/fj.202000508R.

11. Yang, X., Chen, D., Hu, J., Zhao, Q., Fu, X., and Lv, W. (2022). miR-133a-5p inhibits glioma cell proliferation by regulating IGFBP3. JAMA Oncol. *2022*, 8697676. https://doi.org/10.1155/2022/8697676.

12. Xi, Y., Nakajima, G., Hamil, T., Fodstad, O., Riker, A., and Ju, J. (2006). Association of insulin-like growth factor binding protein-3 expression with melanoma progression. Mol. Cancer. Ther. *5*, 3078–3084. https://doi.org/10.1158/1535-7163.MCT-06-0424.

13. Burger, A.M., Leyland-Jones, B., Banerjee, K., Spyropoulos, D.D., and Seth, A.K. (2005). Essential roles of IGFBP-3 and IGFBP-rP1 in breast cancer. Eur. J. Cancer *41*, 1515–1527. https://doi.org/10.1016/j.ejca.2005.04.023.

14. Zhong, Z., Xu, X., Han, S., Shao, Y., and Yi, Y. (2022). Comprehensive analysis of prognostic value and immune infiltration of IGFBP family members in glioblastoma. J. Healthc. Eng. *2022*, 2929695. https://doi.org/10.1155/2022/2929695.

15. Santosh, V., Arivazhagan, A., Sreekanthreddy, P., Srinivasan, H., Thota, B., Srividya, M.R., Vrinda, M., Sridevi, S., Shailaja, B.C., Samuel, C., et al. (2010). Grade-specific expression of insulin-like growth factor-binding proteins-2, -3, and -5 in astrocytomas: IGFBP-3 emerges as a strong predictor of survival in patients with newly diagnosed glioblastoma. Cancer Epidemiol. Biomarkers Prev. *19*, 1399–1408. https://doi.org/10.1158/1055-9965.EPI-09-1213.

16. Chen, C.H., Chen, P.Y., Lin, Y.Y., Feng, L.Y., Chen, S.H., Chen, C.Y., Huang, Y.C., Huang, C.Y., Jung, S.M., Chen, L.Y., and Wei, K.C. (2019). Suppression of tumor growth via IGFBP3 depletion as a potential treatment in glioma. J. Neurosurg. *132*, 168–179. https://doi.org/10.3171/2018.8.JNS181217.

17. Elstner, A., Stockhammer, F., Nguyen-Dobinsky, T.N., Nguyen, Q.L., Pilgermann, I., Gill, A., Guhr, A., Zhang, T., von Eckardstein, K., Picht, T., et al. (2011). Identification of diagnostic serum protein profiles of glioblastoma patients. J. Neuro Oncol. *102*, 71–80. https://doi.org/10.1007/s11060-010-0284-8.

18. Marzec, K.A., Baxter, R.C., and Martin, J.L. (2015). Targeting insulin-like growth factor binding protein-3 signaling in triple-negative breast cancer. BioMed Res. Int. *2015*, 638526. https://doi.org/10.1155/2015/638526.

19. Takaoka, M., Harada, H., Andl, C.D., Oyama, K., Naomoto, Y., Dempsey, K.L., Klein-Szanto, A.J., El-Deiry, W.S., Grimberg, A., and Nakagawa, H. (2004). Epidermal growth factor receptor regulates aberrant expression of insulin-like growth factor-binding protein 3. Cancer Res. *64*, 7711–7723. https://doi.org/10.1158/0008-5472.CAN-04-0715.

20. Butovsky, O., Jedrychowski, M.P., Moore, C.S., Cialic, R., Lanser, A.J., Gabriely, G., Koeglsperger, T., Dake, B., Wu, P.M., Doykan, C.E., et al. (2014). Identification of a unique TGF-beta-dependent molecular and functional signature in microglia. Nat. Neurosci. *17*, 131–143. https://doi.org/10.1038/nn.3599.

21. Chen, Y., Peng, F.F., Jin, J., Chen, H.M., Yu, H., and Zhang, B.F. (2017). Src-mediated ligand release-independent EGFR transactivation involves TGF-beta-induced Smad3 activation in mesangial cells. Biochem. Biophys. Res. Commun. *493*, 914–920. https://doi.org/10.1016/j.bbrc.2017.09.121.

22. Xie, F., Ling, L., van Dam, H., Zhou, F., and Zhang, L. (2018). TGF-beta signaling in cancer metastasis. Acta. Biochim. Biophys. Sin. (Shanghai). *50*, 121–132. https://doi.org/10.1093/abbs/gmx123.

23. Wei, J.W., Cai, J.Q., Fang, C., Tan, Y.L., Huang, K., Yang, C., Chen, Q., Jiang, C.L., and Kang, C.S. (2017). Signal peptide peptidase, encoded by HM13, contributes to tumor progression by affecting EGFRvIII secretion profiles in glioblastoma. CNS Neurosci. Ther. *23*, 257–265. https://doi.org/10.1111/cns.12672.

24. Zhang, X., Wu, A., Fan, Y., and Wang, Y. (2011). Increased transforming growth factor-beta2 in epidermal growth factor receptor variant III-positive glioblastoma. J. Clin. Neurosci. *18*, 821–826. https://doi.org/10.1016/j.jocn.2010.09.024.

25. Baxter, R.C. (2015). Nuclear actions of insulin-like growth factor binding protein-3. Gene *569*, 7–13. https://doi.org/10.1016/j.gene.2015.06.028.

26. Chen, Y.J., Lin, K.N., Jhang, L.M., Huang, C.H., Lee, Y.C., and Chang, L.S. (2016). Gallic acid abolishes the EGFR/Src/Akt/Erk-mediated expression of matrix metalloproteinase-9 in MCF-7 breast cancer cells. Chem. Biol. Interact. *252*, 131–140. https://doi.org/10.1016/j.cbi.2016.04.025.

27. Janowski, E., Jiao, X., Katiyar, S., Lisanti, M.P., Liu, M., Pestell, R.G., and Morad, M. (2011). c-Jun is required for TGF-beta-mediated cellular migration via nuclear Ca(2)(+) signaling. Int. J. Biochem. Cell Biol. *43*, 1104–1113. https://doi.org/10.1016/j.biocel.2011.03.011.

28. Chao, M., Liu, N., Sun, Z., Jiang, Y., Jiang, T., Xv, M., Jia, L., Tu, Y., and Wang, L. (2020). TGF-Beta signaling promotes glioma progression through stabilizing Sox9. Front. Immunol. *11*, 592080. https://doi.org/10.3389/fimmu.2020.592080.

29. Liu, J.Y., Chen, Y.J., Feng, H.H., Chen, Z.L., Wang, Y.L., Yang, J.E., and Zhuang, S.M. (2021). LncRNA SNHG17 interacts with LRPPRC to stabilize c-Myc protein and promote G1/S transition and cell proliferation. Cell Death Dis. *12*, 970. https://doi.org/10.1038/s41419-021-04238-x.

30. Yu, N.T., Ke, F., and Zhang, Q.Y. (2020). Andrias davidianus ranavirus 1R encoding a delayed-early protein promotes cell proliferation by driving cell cycle progression into S phase. Acta Virol. *64*, 10–19. https://doi.org/10.4149/av_2020_102.

31. Zhao, Y., Ma, J., Fan, Y., Wang, Z., Tian, R., Ji, W., Zhang, F., and Niu, R. (2018). TGF-beta transactivates EGFR and facilitates breast

cancer migration and invasion through canonical Smad3 and ERK/Sp1 signaling pathways. Mol. Oncol. *12*, 305–321. https://doi.org/10.1002/1878-0261.12162.

32. Samarakoon, R., Dobberfuhl, A.D., Cooley, C., Overstreet, J.M., Patel, S., Goldschmeding, R., Meldrum, K.K., and Higgins, P.J. (2013). Induction of renal fibrotic genes by TGF-beta1 requires EGFR activation, p53 and reactive oxygen species. Cell. Signal. *25*, 2198–2209. https://doi.org/10.1016/j.cellsig.2013.07.007.

33. Martin, J.L., de Silva, H.C., Lin, M.Z., Scott, C.D., and Baxter, R.C. (2014). Inhibition of insulin-like growth factor-binding protein-3 signaling through sphingosine kinase-1 sensitizes triple-negative breast cancer cells to EGF receptor blockade. Mol. Cancer Ther. *13*, 316–328. https://doi.org/10.1158/1535-7163.MCT-13-0367.

34. Luo, Q., Shi, W., Dou, B., Wang, J., Peng, W., Liu, X., Zhao, D., Tang, F., Wu, Y., Li, X., et al. (2021). XBP1- IGFBP3 signaling pathway promotes NSCLC invasion and metastasis. Front. Oncol. *11*, 654995. https://doi.org/10.3389/fonc.2021.654995.

35. Xue, M., Fang, Y., Sun, G., Zhuo, W., Zhong, J., Qian, C., Wang, L., Wang, L., Si, J., and Chen, S. (2013). IGFBP3, a transcriptional target of homeobox D10, is correlated with the prognosis of gastric cancer. PLoS One *8*, e81423. https://doi.org/10.1371/journal.pone.0081423.

36. Deivendran, S., Marzook, H., Santhoshkumar, T.R., Kumar, R., and Pillai, M.R. (2017). Metastasis-associated protein 1 is an upstream regulator of DNMT3a and stimulator of insulin-growth factor binding protein-3 in breast cancer. Sci. Rep. *7*, 44225. https://doi.org/10.1038/srep44225.

37. Abdolhoseinpour, H., Mehrabi, F., Shahraki, K., Khoshnood, R.J., Masoumi, B., Yahaghi, E., and Goudarzi, P.K. (2016). Investigation of serum levels and tissue expression of two genes IGFBP-2 and IGFBP-3 act as potential biomarker for predicting the progression and survival in patients with glioblastoma multiforme. J. Neurol. Sci. *366*, 202–206. https://doi.org/10.1016/j.jns.2016.05.018.

38. Yen, Y.C., Hsiao, J.R., Jiang, S.S., Chang, J.S., Wang, S.H., Shen, Y.Y., Chen, C.H., Chang, I.S., Chang, J.Y., and Chen, Y.W. (2015). Insulin-like growth factor-independent insulin-like growth factor binding protein 3 promotes cell migration and lymph node metastasis of oral squamous cell carcinoma cells by requirement of integrin beta1. Oncotarget *6*, 41837–41855. https://doi.org/10.18632/oncotarget.5995.

39. Martin, J.L., Weenink, S.M., and Baxter, R.C. (2003). Insulin-like growth factor-binding protein-3 potentiates epidermal growth factor action in MCF-10A mammary epithelial cells. Involvement of p44/42 and p38 mitogen-activated protein kinases. J. Biol. Chem. *278*, 2969–2976. https://doi.org/10.1074/jbc.M210739200.

40. Liu, Q., Jiang, J., Zhang, X., Zhang, M., and Fu, Y. (2021). Comprehensive analysis of IGFBPs as biomarkers in gastric cancer. Front. Oncol. *11*, 723131. https://doi.org/10.3389/fonc.2021.723131.

41. Han, J., Jogie-Brahim, S., Harada, A., and Oh, Y. (2011). Insulin-like growth factor-binding protein-3 suppresses tumor growth via activation of caspase-dependent apoptosis and cross-talk with NF-kappaB signaling. Cancer Lett. *307*, 200–210. https://doi.org/10.1016/j.canlet.2011.04.004.

42. Tian, L., Xie, X., Das, U., Chen, Y., Sun, Y., Liu, F., Lu, H., Nan, P., Zhu, Y., Gu, X., et al. (2022). Forming cytoplasmic stress granules PURalpha suppresses mRNA translation initiation of IGFBP3 to promote esophageal squamous cell carcinoma progression. Oncogene *41*, 4336–4348. https://doi.org/10.1038/s41388-022-02426-3.

43. Rosendahl, A.H., Hietala, M., Henningson, M., Olsson, H., and Jernström, H. (2011). IGFBP1 and IGFBP3 polymorphisms predict circulating IGFBP-3 levels among women from high-risk breast cancer families. Breast Cancer Res. Treat. *127*, 785–794. https://doi.org/10.1007/s10549-010-1277-1.

44. Neftel, C., Laffy, J., Filbin, M.G., Hara, T., Shore, M.E., Rahme, G.J., Richman, A.R., Silverbush, D., Shaw, M.L., Hebert, C.M., et al. (2019). An integrative model of cellular states, plasticity, and genetics for glioblastoma. Cell *178*, 835–849.e21. https://doi.org/10.1016/j.cell.2019.06.024.

45. Fu, W., Wang, W., Li, H., Jiao, Y., Huo, R., Yan, Z., Wang, J., Wang, S., Wang, J., Chen, D., et al. (2020). Single-cell Atlas reveals complexity of the immunosuppressive microenvironment of initial and recurrent glioblastoma. Front. Immunol. *11*, 835. https://doi.org/10.3389/fimmu.2020.00835.

46. Kumar, R., Gont, A., Perkins, T.J., Hanson, J.E.L., and Lorimer, I.A.J. (2017). Induction of senescence in primary glioblastoma cells by serum and TGFbeta. Sci. Rep. *7*, 2156. https://doi.org/10.1038/s41598-017-02380-1.

47. Gong, L., Ji, L., Xu, D., Wang, J., and Zou, J. (2021). TGF-beta links glycolysis and immunosuppression in glioblastoma. Histol. Histopathol. *36*, 1111–1124. https://doi.org/10.14670/HH-18-366.

48. Nickl-Jockschat, T., Arslan, F., Doerfelt, A., Bogdahn, U., Bosserhoff, A., and Hau, P. (2007). An imbalance between Smad and MAPK pathways is responsible for TGF-beta tumor promoting effects in high-grade gliomas. Int. J. Oncol. *30*, 499–507.

49. Dong, L.M., Brennan, P., Karami, S., Hung, R.J., Menashe, I., Berndt, S.I., Yeager, M., Chanock, S., Zaridze, D., Matveev, V., et al. (2009). An analysis of growth, differentiation and apoptosis genes with risk of renal cancer. PLoS One *4*, e4895. https://doi.org/10.1371/journal.pone.0004895.

50. Lin, M.Z., Marzec, K.A., Martin, J.L., and Baxter, R.C. (2014). The role of insulin-like growth factor binding protein-3 in the breast cancer cell response to DNA-damaging agents. Oncogene *33*, 85–96. https://doi.org/10.1038/onc.2012.538.

51. Yamaoka, T., Ohmori, T., Ohba, M., Arata, S., Murata, Y., Kusumoto, S., Ando, K., Ishida, H., Ohnishi, T., and Sasaki, Y. (2017). Distinct afatinib resistance mechanisms identified in lung adenocarcinoma harboring an EGFR mutation. Mol. Cancer Res. *15*, 915–928. https://doi.org/10.1158/1541-7786.MCR-16-0482.

52. Sharieh, E.A., Awidi, A.S., Ahram, M., and Zihlif, M.A. (2016). Alteration of gene expression in MDA-MB-453 breast cancer cell line in response to continuous exposure to Trastuzumab. Gene *575* (2 Pt 2), 415–420. https://doi.org/10.1016/j.gene.2015.09.019.

53. Vaubel, R.A., Tian, S., Remonde, D., Schroeder, M.A., Mladek, A.C., Kitange, G.J., Caron, A., Kollmeyer, T.M., Grove, R., Peng, S., et al. (2020). Genomic and phenotypic characterization of a broad panel of patient-derived xenografts reflects the diversity of glioblastoma. Clin. Cancer Res. *26*, 1094–1104. https://doi.org/10.1158/1078-0432.CCR-19-0909.

54. Wu, S., Gao, F., Zheng, S., Zhang, C., Martinez-Ledesma, E., Ezhilarasan, R., Ding, J., Li, X., Feng, N., Multani, A., et al. (2020). EGFR amplification induces increased DNA damage response and renders selective sensitivity to talazoparib (PARP inhibitor) in glioblastoma. Clin. Cancer Res. *26*, 1395–1407. https://doi.org/10.1158/1078-0432.CCR-19-2549.

55. Zheng, Q., Han, L., Dong, Y., Tian, J., Huang, W., Liu, Z., Jia, X., Jiang, T., Zhang, J., Li, X., et al. (2014). JAK2/STAT3 targeted therapy suppresses tumor invasion via disruption of the EGFRvIII/JAK2/STAT3 axis and associated focal adhesion in EGFRvIII-expressing glioblastoma. Neuro Oncol. *16*, 1229–1243. https://doi.org/10.1093/neuonc/nou046.

STAR★METHODS

KEY RESOURCES TABLE

REAGENT or RESOURCE	SOURCE	IDENTIFIER
Antibodies		
Rabbit mAb anti-p-EGFR (Tyr1068) (D7A5)	Cell Signaling Technology	Cat#3777; RRID: AB_2096270
Rabbit mAb anti-c-Jun (60A8)	Cell Signaling Technology	Cat#9165; RRID: AB_2130165
Rabbit mAb anti-p-Akt (Ser473)	Cell Signaling Technology	Cat#4060; RRID: AB_2315049
Rabbit mAb anti-AKT	Cell Signaling Technology	Cat#4685; RRID: AB_2225340
Rabbit mAb anti-p-Erk1/2 (Thr202/Tyr204)	Cell Signaling Technology	Cat#4370; RRID: AB_2315112
Rabbit mAb anti-ERK1/2	Cell Signaling Technology	Cat#4695; RRID: AB_390779
Rabbit mAb anti-p-Smad2	Cell Signaling Technology	Cat#18338; RRID: AB_2798798
Rabbit mAb anti-p-Smad3	Cell Signaling Technology	Cat#9520; RRID: AB_2193207
Rabbit mAb anti-Smad2/3	Cell Signaling Technology	Cat#5678; RRID: AB_10693547
Mouse mAb anti-β-actin	Cell Signaling Technology	Cat#3700; RRID: AB_2242334
Mouse mAb anti-EGFR cocktail	Invitrogen	Cat#AHR5062; RRID: AB_2536360
Rabbit pAb anti-IGFBP3	Proteintech	Cat#10189-2-AP; RRID: AB_2123233
Mouse mAb anti-LaminB1	Proteintech	Cat#66095-1-Ig; RRID: AB_11232208
Rabbit pAb anti-β-tubulin	Proteintech	Cat#10094-1-AP; RRID: AB_2210695
Mouse mAb anti-CDK2	Proteintech	Cat#60312-1-AP; RRID: AB_2881424
Rabbit pAb anti-Cyclin E1	Proteintech	Cat#11554-1-AP; RRID: AB_2071066
Rabbit pAb anti-Cyclin E2	Proteintech	Cat#11935-1-AP; RRID: AB_2228593
Anti-rabbit IgG, HRP-linked Antibody	Proteintech	Cat#SA00001-2-AP; RRID: AB_2722564
Anti-mouse IgG, HRP-linked Antibody	Proteintech	Cat#SA00001-1-AP; RRID: AB_2722565
Rabbit pAb anti-Ki-67	Proteintech	Cat#27309-1-AP; RRID: AB_2756525
Rabbit pAb anti-CD31	Proteintech	Cat#11265-1-AP; RRID: AB_2299349
Rabbit mAb anti-EGFRvIII (D6T2Q)	Cell Signaling Technology	Cat#64952, RRID: AB_2773018
Rabbit mAb anti-TGF-β1	Abcam	Cat#ab179695; Clone: EPR18163
Mouse IgG	Beyotime Biotechnology	Cat#A7028; RRID: AB_2909433
Bacterial and virus strains		
Psi-LvRU6rLP-red firefly luciferase-shControl	GeneCopoeia	LPP-CSHCTR001-LvRU6rLP-100
Psi-LvRU6rLP-red firefly luciferase-shIGFBP3	GeneCopoeia	LPP-HSH009545-LvRU6rLP-01-200
Biological samples		
Human glioma tissue microarray	Shanghai Outdo Biotech Co., Ltd. (SOBC)	HBraG080PG01

(*Continued on next page*)

Continued

REAGENT or RESOURCE	SOURCE	IDENTIFIER
Chemicals, peptides, and recombinant proteins		
Human TGF-β	PeproTech	Cat#AF-100-21C-10UG
U0126 MEK inhibitor	Selleckchem	Cat#S1102
LY294002 PI3K inhibitor	Selleckchem	Cat#S1105
LY2157299 TGF-βR inhibitor	Selleckchem	Cat#S2230
Matrigel	Corning	Cat#354230
RIPA Lysis Buffer	Sigma-Aldrich	Cat#R0278
NE-PER™ Nuclear and Cytoplasmic Extraction reagents	ThermoFisher	Cat#78833
ECL reagent	Millipore	Cat#WBKLS0500
TRIzol reagent	Invitrogen	Cat#15596018
Lipofectamine 2000 Transfection Reagent	Invitrogen	Cat#11668019
Non-fat milk	Seven	Cat#SW128-02
Phenylmethanesulfonyl fluoride (PMSF)	Beyotime Biotechnology	Cat#ST505
Crystal violet	Sigma-Aldrich	Cat#V5265
Protein A/G-agarose	Abmart	Cat#A10001H
In vivo-jetPEI transfection reagent	Polyplus transfection	Cat#101000040
Triton X-100	Sigma-Aldrich	Cat#T8200
2-(4-Amidinophenyl)-6-indolecarbamidine dihydrochloride (DAPI)	Beyotime Biotechnology	Cat#C1002
Tween 20	Beyotime Biotechnology	Cat#ST825-100mL
TBS	Beyotime Biotechnology	Cat#P0228
SDS–PAGE	Beyotime Biotechnology	Cat#P0014A
Leptomycin B (LMB)	Beyotime Biotechnology	Cat#S1726-50 μg
Critical commercial assays		
SYBR Green PCR kit	Roche	Cat#QR0100
Human IGFBP3 ELISA kits	Raybiotech	Cat#ELH-IGFBP3
High Capacity cDNA Reverse Transcription Kit	Applied Biosystems	Cat#4368814
Dual Luciferase Reporter Gene Assay Kit	GenePharma	N/A
BCA assay kit	Solarbio	Cat#PCG0020
Cell cycle assay kit	Solarbio	Cat#CA1510
DAB kit	Gene tech	Cat#GK600505
Experimental models: Cell lines		
Human: U87-MG	ATCC	HTB-14
Human: LN229	ATCC	CRL-2611
Human: U87-vector; U87-EGFRvIII	(Zheng, Q.F., et al., 2014)[55]	N/A
Human: LN229-vector; LN229-EGFRvIII	(Zheng, Q.F., et al., 2014)[55]	N/A
Experimental models: Organisms/strains		
BALB/c nude mice (five-week-old, female)	Beijing SiPeiFu	N/A
Oligonucleotides		
siRNA targeting sequence: Scr: UAACGACGCGACGACGUAA;	GenePharma	N/A
siRNA targeting sequence: IGFBP3: CAGAGCACAGAUACCCAGAACUUCU;	GenePharma	N/A
siRNA targeting sequence: c-Jun: UGGGAGAGGCAUCAUCGAATT;	GenePharma	N/A

(*Continued on next page*)

Continued

REAGENT or RESOURCE	SOURCE	IDENTIFIER
shRNA targeting sequence: Control: TTCTCCGAACGTGTCACGTTT	GeneCopoeia	N/A
shRNA targeting sequence: IGFBP3: CAGAGCACAGATACCCAGAACTTCT	GeneCopoeia	N/A
Primers for Real-time PCR, see Table S1	This paper	N/A
Recombinant DNA		
Plasmid: pcDNA3.1(+)-c-Jun	GenePharma	N/A
Plasmid: GPL3-Basic-IGFBP3-WT	GenePharma	N/A
Plasmid: GPL3-Basic-IGFBP3-Mut	GenePharma	N/A
Software and algorithms		
ImageJ	ImageJ Software	https://imagej.nih.gov/ij/
GraphPad Prism 8.0	GraphPad Software	https://www.graphpad.com/
SPSS 19.0	SPSS	http://www.spss.com.cn

RESOURCE AVAILABILITY

Lead contact

Further information and requests for resources and reagents should be directed to and will be fulfilled by the lead contact, Yucui Dong (yucuidong@bzmc.edu.cn).

Materials availability

The cell lines and plasmids that were generated in this study will be available upon reasonable request.

Data and code availability

- All the detailed data in this paper are available upon request. Original western blot images have been deposited at Mendeley and are publicly available as of the date of publication.
- This paper does not report original code.
- Any additional information required to reanalyze the data reported in this paper is available from the lead contact upon request.

EXPERIMENTAL MODEL AND SUBJECT DETAILS

Tissue microarray

The human tissue microarray studies were conducted in accordance with the Declaration of Helsinki, and approved by the Ethics Committee of Shanghai Outdo Biotech Co., Ltd. (SOBC).

Cell lines and cell culture

Human glioblastoma cell lines U87MG, LN229 were obtained from the AmericanType Culture Collection (ATCC) (Manassas, VA, USA). The obtainment of human GBM cell lines (U87-vector; U87-EGFRvIII; LN229-vector; LN229-EGFRvIII) was the same as our previous described.[55] These cells were maintained in DMEM (Sigma-Aldrich, StLouis, MO, USA) containing 400 μg/mL G418, 10% fetal bovine serum (FBS, vistech) and 1% penicillin/streptomycin at 37°C with 5% CO_2.

Stable knockdown of IGFBP3 in U87-EGFRvIII cells: U87-EGFRvIII cells were transduced at 70%-80% density with purified shControl lentiviral particles (psi-LvRU6rLP-red firefly luciferase-shControl, GeneCopoeia) and purified shIGFBP3 lentiviral particles (psi-LvRU6rLP-red firefly luciferase-shIGFBP3, GeneCopoeia). After 72 h, transduced U87-EGFRvIII cells were maintained under 1 μg/mL puromycin (Sigma-Aldrich) selection. The down-regulation of IGFBP3 was detected by western blotting.

Nude mouse glioma subcutaneous model and intracranial model

The animal research was performed according to the internationally recognized guidelines and national regulations. The animal study was reviewed and approved by Binzhou Medical University Ethics Committee. Mice were housed in sterile cages and housed in SPF animal rooms on a 12-hour light-dark cycle. All the animals were fed water and standard mouse diet as they pleased. For flank tumor implantation, mice were comforted and injected in the back with a syringe.

To establish a subcutaneous model, cells were treated with *IGFBP3*-siRNA and *Control*-siRNA in advance *in vitro*. Five-week-old female BALB/c nude mice (SiPeiFu, Beijing, China) were randomly divided into 2 groups with 6 mice in each group, and were injected with 5×10^6/100 μL U87-EGFRvIII-si-*Control* and U87-EGFRvIII-si-*IGFBP3* cells, respectively. *IGFBP3* siRNA of 10 μg/mouse were mixed with *in vivo* jetPEI transfection reagent (Polyplus transfection, Strasbourg, France) according to the manufacturer's instruction and infused into intratumoral. The jetPEI mixture was injected every two days, and mouse body weight and tumor volume were measured before injection. Sizes of tumors were detected via a vernier caliper with tumor volume:0.5 × length × width^2.

To monitor mice survival, an intracranial model was established. 1×10^6/10 μL U87-EGFRvIII-shControl and U87-EGFRvIII-shIGFBP3 cells were injected into the intracranial striatum (n = 10 per group) at a depth of 3.0 mm using stereotactic instrument, respectively. The mice were taken care of normally during the tumorigenesis period and the survival time was observed. The mice were anesthetized and euthanized when they had lost more than 20% to 25% of their body weight, a moribund state or unable to eat normally.

METHOD DETAILS

Reagents

Cytokine TGF-β purchased from PeproTech (Beijing, China). The molecular-targeted inhibitors, MTT reagent and Leptomycin B (LMB) were purchased from Beyotime (Haimen, Jiangsu, China). All inhibitors were dissolved in dimethyl sulfoxide (DMSO) and stored in optimum concentration according to their instructions.

Cell proliferation assay

Cells were planted in a 96-well plate with 5×10^3 cells/well. The cells were treated with the 10 ng/mL TGF-β for 24 h and 48 h, respectively. MTT reagent (0.5 mg/mL) was added to each well and incubated for 4 h, after which time the supernatants were removed and the formazan crystals were dissolved in dimethyl sulfoxide. The absorbance was measured at 490 nm with a microplate reader.

Cell cycle analysis

The cells were collected and fixed with 70% precooled ethanol and incubated at 4°C overnight. RNaseA and propidium iodide (PI) were added to the cell precipitate according to the reagent manufacturer's instructions (Solarbio, Beijing, China) for DNA staining. Flow cytometry was performed, and cell cycle was analyzed by Modfit software to determine cell cycle distribution.

Cell invasion assay

Cell invasion was determined using transwell chambers with an 8 μm pore size (Corning, NY, USA). While 4×10^4 GBM cells were seeded in 100 μL serumfree medium in the upper chamber. The lower chamber was filled with 600 μL of medium containing 5% fetal bovine serum. After 48 hours of incubation, matrigel and cells in the upper chamber were removed. The cells on the lower surface were stained with 1% crystal violet (Sigma-Aldrich) and counted in 6 randomly selected fields to quantify the cell invasion rates.

Wound-healing assay

The GBM cells were planted into 6-well plates at 70%-80% confluence. Confluent cells were wounded by a 10-μL pipette tip, TGF-β was added and incubated for 24 h or 48 h. Wound healing was observed, and representative scrape lines were photographed. Counted in 6 randomly selected fields to quantify the relative cell migration rates with or without treatment.

siRNA transfection

Negative control siRNA and siRNA targeting at either of *IGFBP3* and *c-Jun* (Genepharma, Shanghai, China) were transfected into EGFRvIII-expressing GBM cells or vector cells using Lipofectamine 2000 (Invitrogen, Carlsbad, CA, USA) according to the manufacturer's instructions. si-*Scr*, sense: (5′-UAACGACGCGAC GACGUAA-3′); si-*IGFBP3*, sense: (5′-CAGAGCACAGAUACCCAGAACUUCU-3′); si-*c-Jun*, sense: (5′-UGG GAGAGGCAUCAUCGAATT-3′). QRT-PCR and western blotting assays 48 hours post transfection were used to detect the efficiency of *IGFBP3* siRNA and *c-Jun* siRNA. The following shRNAs were used: Control shRNA oligonucleotide, 5′-TTCTCCGAACGTGTCACGTTT-3′; IGFBP3 shRNA oligonucleotide, 5′-CAGA GCACAGATACCCAGAACTTCT-3′.

Western blot assay and immunoprecipitation

Whole-cell lysates were harvested using cell lysis buffer which containing protease inhibitors and phosphatase inhibitors. Nuclear and cytoplasmic fractions were prepared using NE-PER reagents according to the manufacturer's instructions (Thermo Scientific, Waltham, MA, USA). Protein concentrations were determined by BCA assay (Solarbio, Beijing, China). 30 μg total protein was isolated by 10% SDS-PAGE and transferred to PVDF membrane. The non-specific reactivity was blocked with nonfat milk for 2 h at room temperature. The PVDF membranes were then incubated with primary antibodies at 4°C overnight. After washing with TBST, HRP labeled sheep anti-rabbit and sheep anti-mouse secondary antibodies were incubated for 2 h. Enhanced chemiluminescence system (ECL) was used to visualize and grayscale analysis was performed using ImageJ software. For immunoprecipitation, U87-EGFRvIII cells (1×10^6) were treated with ice-cold RIPA buffer (Sigma-Aldrich), and the cells were disrupted by repeated pipetting. 1 μg of antibody was added to 1 mg of the protein lysate, after 4 h incubation at 4°C and 30 μL of protein A/G-agarose (Abmart, Shanghai, China) was added. The samples were then incubated overnight at 4°C. After washing with cold RIPA buffer and the immunoprecipitated proteins were eluted. Western blotting was carried out as described above.

Primary antibodies including anti-p-EGFR (#3777, RRID: AB_2096270), c-Jun (#9165, RRID: AB_2130165), β-actin (#3700, RRID: AB_2242334), p-AKT (#4060, RRID: AB_2315049), AKT (#4685, RRID: AB_2225340), p-ERK1/2 (#4370, RRID: AB_2315112), ERK1/2 (#4695, RRID: AB_390779), p-Smad2 (#18338, RRID: AB_2798798), p-Smad3 (#9520, RRID: AB_2193207), Smad2/3 (#5678, RRID: AB_10693547) at 4°C overnight. All antibodies are purchased from Cell Signaling Technology (CST, Danvers, MA, USA), except the EGFR antibody cocktail (Cat No. AHR5062, RRID: AB_2536360) which was purchased from Invitrogen and IGFBP3 antibody (Cat No. 10189-2-AP, RRID: AB_2123233) which was purchased from Proteintech (Proteintech, USA). Cell cyclin-related proteins CDK2 (Cat No. 60 312-1-AP, RRID: AB_2881424), Cyclin E1 (Cat No. 11554-1-AP, RRID: AB_2071066) and Cyclin E2 (Cat No. 11935-1-AP, RRID: AB_2228593) were purchased from Proteintech. TGF-β (Cat No. 179695) was purchased from Abcam (Waltham, MA, USA). IgG (Cat#A7028; RRID: AB_2909433) was purchased from Beyotime. The following secondary antibodies were used: HRP labeled sheep anti-rabbit (Cat No. SA00001-2, RRID: AB_2722564) and sheep anti-mouse (Cat No. SA00001-1, RRID: AB_2722565).

Quantitative RT-PCR

Total RNA was extracted using Trizol reagent (Invitrogen) according to manufacturer's instructions, and the concentration of extracted RNA was measured using an ultramicro nucleic acid protein analyzer. cDNA was reverse-transcribed from 1 μg RNA with a High Capacity cDNA Reverse Transcription Kit (Applied Biosystems, Foster city, CA, USA). The FastStart Universal SYBR Green Master (ROX) (Roche) Assay Kit was used for qRT-PCR to detect the expression of different genes. Fold-changes in relative gene expression were calculated by the comparative Ct method (fold change = $2^{-\triangle\triangle Ct}$). Primer sequences are listed in Supplementary information (Table S1).

ELISA

Culture medium was collected and subjected to ELISA analysis. The GBM cells at logarithmic growth stage were cultured in a 12-well plate. Human IGFBP3 concentration were measured by ELISA (Raybiotech, Norcross, GA, USA) according to the manufacturer's protocols.

Immunofluorescence

Cells were grown on glass cover slips in 12-well plates before fixed with 4% paraformaldehyde. Permeabilized with 0.1% Triton X-100 for 15 min, and blocked with 10% normal goat serum for 1 hour. The coverslips

incubation with the primary antibody at a 1:100 dilution overnight at 4°C. FITC-or Alexa fluor-labeled anti-rabbit or anti-mouse antibody was added to the incubation. The nuclei were stained with DAPI (Beyotime). The samples were observed under ZEISS LSM 510 META confocal microscope (Carl Zeiss, Jena, Germany) and all images were captured using a 63×oil immersion objective (Plan-Apochromat 63×/1.40 Oil DIC M27).

Luciferase report assay

The c-Jun sequence was cloned into pcDNA3.1(+), and the conserved sequences of wild-IGFBP3 and Mut-IGFBP3 promoters were cloned into GPL3-Basic vector. The luciferase assay was conducted using dual luciferase reporter assay (Genepharma, Shanghai, China) according to the manufacturer's instructions. The promoter activity was calculated from the chemical luminescence intensity ratio of firefly.

Immunohistochemistry (IHC)

Histological sections of the tumor tissue were fixed in 10% neutral buffered formalin for IHC analysis. The sections were incubated at 4°C overnight in a 1:100 dilution with primary antibodies anti-IGFBP3, -EGFRvIII (#64952, RRID: AB_2773018), -Ki-67 (Cat No. 27309-1-AP; RRID: AB_2756525) and -CD31 (Cat No. 11265-1-AP, RRID: AB_2299349), before being incubated with a biotin-labeled secondary antibody (1:100) for 1 h at 37°C, and finally stained with diaminobenzidine (DAB) and hematoxylin; the sections were then counter-stained with hematoxylin and mounted. The images were captured with Olympus IX81 microscopy.

Conditioned medium (CM) preparation

The medium from 10^6 cells yielded 4 mL of primary CM, which was further de-salted and concentrated 80-fold by centrifugation (4000 × g for 20 min at 4°C) using ultrafiltration units with a 10-kDa molecular weight cutoff (Amicon Ultra-4; Millipore, Billerica, MA, USA), yielding 200 μL of concentrated CM. Serum-free DMEM (de-salted and concentrated 80-fold) served as a vehicle control.

QUANTIFICATION AND STATISTICAL ANALYSIS

All experiments *in vitro* were repeated at least three times. Statistical analysis was performed using the SPSS 19.0 software, which was expressed as mean ± standard deviation (SD). Student's t-test was performed to compare the means of values from different experiments, and ANOVA was used to investigate the differences in multiple groups. Spearman's rank correlation determined the association between IGFBP3 protein and EGFRvIII protein. Overall survival rate was analyzed using the Kaplan–Meier plot and tested via the log rank test. Differences were considered statistically significant at $p < 0.05$*, $p < 0.01$**, $p < 0.001$***.